Quaternary Science Reviews 43 (2012) 16–32

Contents lists available at SciVerse ScienceDirect

Quaternary Science Reviews

journal homepage: www.elsevier.com/locate/quascirev

The Medieval Climate Anomaly in the Iberian Peninsula reconstructed from marine and lake records

Ana Moreno [a,b,*], Ana Pérez [a], Jaime Frigola [c], Vanesa Nieto-Moreno [d], Marta Rodrigo-Gámiz [d,e], Belén Martrat [f], Penélope González-Sampériz [a], Mario Morellón [g], Celia Martín-Puertas [h], Juan Pablo Corella [a,i], Ánchel Belmonte [j], Carlos Sancho [j], Isabel Cacho [c], Gemma Herrera [c], Miquel Canals [c], Joan O. Grimalt [f], Francisco Jiménez-Espejo [d], Francisca Martínez-Ruiz [d], Teresa Vegas-Vilarrúbia [k], Blas L. Valero-Garcés [a,b]

[a] *Instituto Pirenaico de Ecología (CSIC), Zaragoza, Spain*
[b] *Laboratorio Internacional de Cambio Global (LINCGlobal), Departamento de Ecologıa, Facultad de Ciencias Biológicas, PUC, Santiago, Chile*
[c] *GRC Marine Geosciences, Universidad de Barcelona, Barcelona, Spain*
[d] *Instituto Andaluz de Ciencias de la Tierra (CSIC-UGR), Armilla, Granada, Spain*
[e] *Department of Marine Organic Biogeochemistry, Royal Netherlands Institute for Sea Research (NIOZ), Texel, The Netherlands*
[f] *Department of Environmental Chemistry, Institute of Environmental Assessment and Water Research (IDÆA), Spanish Council for Scientific Research (CSIC), Barcelona, Spain*
[g] *Department of Surface Waters – Eawag, Dübendorf, Switzerland*
[h] *German Research Center for Geoscience (GFZ), Potsdam, Germany*
[i] *Institut des Sciences de l'Environnement (ISE), Dept of Geology and Paleontology, University of Geneva, 1205 Genève, Switzerland*
[j] *Department of Earth Sciences, University of Zaragoza, Zaragoza, Spain*
[k] *Department of Ecology, Faculty of Biology, University of Barcelona, Barcelona, Spain*

A R T I C L E I N F O

Article history:
Received 3 August 2011
Received in revised form
4 April 2012
Accepted 5 April 2012
Available online xxx

Keywords:
Medieval Climate Anomaly
Iberian Peninsula
Lacustrine sediments
Marine cores
North Atlantic Oscillation

A B S T R A C T

Selected multi-proxy and accurately dated marine and terrestrial records covering the past 2000 years in the Iberian Peninsula (IP) facilitated a comprehensive regional paleoclimate reconstruction for the Medieval Climate Anomaly (MCA: 900–1300 AD). The sequences enabled an integrated approach to land–sea comparisons and, despite local differences and some minor chronological inconsistencies, presented clear evidence that the MCA was a dry period in the Mediterranean IP. It was a period characterized by decreased lake levels, more xerophytic and heliophytic vegetation, a low frequency of floods, major Saharan eolian fluxes, and less fluvial input to marine basins. In contrast, reconstruction based on sequences from the Atlantic Ocean side of the peninsula indicated increased humidity. The data highlight the unique characteristics of the MCA relative to earlier (the Dark Ages, DA: ca 500–900 years AD) and subsequent (the Little Ice Age, LIA: 1300–1850 years AD) colder periods. The reconstruction supports the hypothesis of Trouet et al. (2009), that a persistent positive mode of the North Atlantic Oscillation (NAO) dominated the MCA.

1. Introduction

The combination of proxy records from several paleoclimate archives (including tree rings, lake sediments, marine cores and speleothems) has enabled identification of five climatic periods during the last two millennia. These have been characterized in terms of temperature and precipitation variability (Mann and Jones, 2003), and include: the Roman Warm Period (RWP; 0–500 years AD), the Dark Ages (DA; 500–900 AD), the Medieval Warm Period (MWP; 900–1300 AD), the Little Ice Age (LIA; 1300–1850 AD), and a subsequent period of warming. Thus, the MWP, which is also termed the Medieval Climate Anomaly (MCA) because of its large heterogeneity in space and time, is the most recent pre-industrial warm era in European climatology (Mann et al., 2009). Although the rates of temperature change (approximately 0.25 °C/100 years in the MCA *vs.* 2–6 °C/100 years at present) and the forcing mechanisms (natural *vs.* anthropogenic) (Solomon et al., 2007) were probably very different during the MCA relative to those under the current conditions of global warming, in both cases the ecosystem and human societies faced new environmental changes. Our understanding of the dynamics and impact of present-day global change will be enhanced from studies of past analogues of periods of abrupt change, and also from comparison

* Corresponding author. Instituto Pirenaico de Ecología (CSIC), Zaragoza, Spain.
E-mail address: amoreno@ipe.csic.es (A. Moreno).

0277-3791/$ – see front matter © 2012 Elsevier Ltd. All rights reserved.
doi:10.1016/j.quascirev.2012.04.007

with previous warmer periods that were characterized by more gradual changes, such as the MCA. To adapt to and mitigate the effects of present-day global warming it is crucial to understand the causes of the MCA and its forcing factors. Better characterization of temperature and precipitation changes that occurred at a large number of sites located in geographically diverse areas is required to corroborate the global character of the MCA and its spatial variability. To date, the MCA has been mainly described by temperature reconstructions that did not provide a worldwide coverage (Jones et al., 2009).

Climate variability during the last millennium has been related to fluctuations in solar irradiance amplified by feedback mechanisms including ozone production or changes in cloud formation (Gray et al., 2010). Thus, in response to greater solar irradiance during the MCA, persistent La Niña-like tropical Pacific Ocean conditions (Mann et al., 2009), a warm phase of the Atlantic Multidecadal Oscillation (AMO), and a more recent positive phase of the North Atlantic Oscillation (NAO) (Trouet et al., 2009) have been reconstructed in attempts to explain the observed worldwide hydroclimate variability during this period (Seager et al., 2007). The NAO signature appears to be particularly evident in climate reconstructions from Scottish stalagmites (wet during the MCA) (Proctor et al., 2002) and from tree rings from Morocco (dry during the MCA) (Esper et al., 2007); in both cases a positive NAO index was likely to have been a major forcing factor, as suggested by Trouet et al. (2009).

Reconstructions of precipitation variability during the MCA are particularly challenging (Seager et al., 2007), and are much rarer than those of temperature. However, the impacts of climate warming on the hydrological cycle are of paramount importance in the Mediterranean region, which is a densely populated area characterized by a permanent water deficit, and is likely to be subject to extreme hydrological events (particularly droughts) in coming decades (Giorgi, 2006). Within the Mediterranean Basin the Iberian Peninsula (IP) (which is located at the southern edge of the storm tracks that are associated with mid-latitude westerly winds and largely controlled by the NAO and the AMO) is a location uniquely placed for exploration of the influence of the long-term NAO index and the Atlantic Ocean dynamics on hydrological variability.

The study of sedimentary records from small lakes, in which considerable fluctuations in lake levels, water chemistry and biological processes controlled by changes in effective moisture have occurred (Last and Smol, 2001), appears to be the best approach to investigating the impact of the MCA on the hydrological cycle in the IP. Other terrestrial records, such as those in speleothems, provide good information on past temperature conditions. Thus, a recent study of three caves in northern Spain indicated that warmer conditions occurred during the MCA (Martín-Chivelet et al., 2011). Marine sediments in the vicinity of the IP also provide evidence of changes in sea surface temperature (SST), river sediment delivery, and wind patterns related to climate changes during the last millennium (Abrantes et al., 2005; Lebreiro et al., 2006). A review of rapid climate change events during the Holocene (Fletcher and Zielhofer, in press) has shown that in several IP records there is clear evidence of contrasting humidity conditions during the MCA and the LIA. Comparison of marine and terrestrial records provides an integrative approach to the reconstruction of climate variability during past centuries.

The purpose of this study was to review recently published and new Iberian paleoenvironmental records for the last two millennia that fulfil the following requisites: (1) the paleoclimate interpretations were based on multi-proxy reconstructions; and (2) the chronology was independent, based on calibrated accelerator mass spectrometry (AMS) ^{14}C dates and $^{137}Cs/^{210}Pb$ models. Based on available records for the IP (Table 1, Fig. 1) we undertook the first synthesis of the environmental response in the region during the MCA (900–1300 AD), and characterized and integrated the signals recorded from the marine and terrestrial realms.

2. Study sites: current climatic and oceanographic setting

The current climate of the IP is mainly driven by the position of the Azores high pressure system. The weather in summer is usually dry and hot because of the influence of the atmospheric subtropical high pressure belt (Sumner et al., 2001). During winter the subtropical high shifts to the south, enabling mid-latitude storms to enter the region from the Atlantic Ocean, which brings rainfall to the IP. As a consequence of the geographic situation and topographic conditions, the climate of the IP is extremely diverse but can be roughly divided into three main climatic areas (Fig. 1): (i) the inland areas having a moderate continental climate; (ii) the Mediterranean climate region; and (iii) the oceanic (Atlantic Ocean) climate of the north and northwest of the IP. In addition, some of the higher altitude areas (including the Pyrenees, Sierra Nevada and Iberian Range) have a mountainous (alpine) climate. Both geography and climate are critical influences on the distribution of vegetation, and determine the biogeographical features of the Euro-Siberian and Mediterranean regions (Blanco-Castro et al., 1997; Rivas-Martínez, 2007).

At a decadal scale climate variability over western Europe is strongly influenced by the NAO (Trigo et al., 2004; Vicente-Serrano and López-Moreno, 2006). According to recent studies the NAO explains 21%, 28% and 33% of total atmospheric circulation variability in spring, autumn and winter, respectively (Trigo and Palutikof, 2001). A very positive NAO index results from a strong meridional pressure gradient that forces the North Atlantic depression to follow a more northerly route, which produces wetter winters over northern Europe (Scandinavia, Scotland and Iceland) and drier winters over southern Europe and northern Africa (Wanner et al., 2001; Trigo et al., 2002). A very negative NAO index is associated with a southward displacement of the storm tracks, which leads to more rainfall in southern latitudes. This was the case in winter 2010, when the IP (particularly the western and southern areas) received historically unprecedented levels of precipitation (Vicente-Serrano et al., 2011). In contrast to the Atlantic Ocean sources of precipitation, localized precipitation, and particularly that resulting from Mediterranean influences, is unrelated to the NAO but shows a moderate correlation with the ENSO (Rodó et al., 1997). Martín-Vide and López-Bustins (2006) investigated sea level pressure differences between the Gulf of Cadiz and northern Italy, and defined the Western Mediterranean Oscillation index (WeMOi); when this is in a positive phase there is a decrease of precipitation in the eastern IP. These studies all highlight the complexity of the IP climate.

From an oceanographical point of view the IP lies in the recirculation regime linking the Gulf Stream with the North Equatorial current *via* the Portuguese–Canary boundary current, which flows north to south along the western Iberian margin and favours the upwelling of cold and nutrient-rich intermediate waters (Fiúza, 1983). A branch of that current enters the western Mediterranean Sea through the Strait of Gibraltar, and mixes at the surface with the Mediterranean Surface Water (MSW), forming the Modified Atlantic Water (MAW) as the water becomes saltier and denser. The semi-enclosed character of the Mediterranean Sea leads to a complete thermohaline circulation system, involving the entry of the MAW, *in situ* densification by air–sea interaction, and deep outflowing to the Atlantic Ocean through the Alboran Sea (Pinardi and Masetti, 2000). The Western Mediterranean Deep Water (WMDW) is produced in the Gulf of Lion (Fig. 1) by evaporation and

Table 1
Lake and marine records from the IP that were reviewed in this paper, organized from north to south and from west to east (see Fig. 1). The signal reconstructed for the MCA is indicated by vegetation cover and climate characteristics. References to previously published data are indicated where applicable.

Site	Coordinates (with altitude or bathymetry)	Lake/ Marine site	MCA signal		References
			Vegetation	Hydrology/Climate	
Northern Iberia					
Ría de Vigo cores	42°14′N; 8°47′W; 45 m bsl	Shallow marine	Deciduous oak woodlands with heaths and substantial prairies. Increase in temperate trees and total pollen influx, suggesting a **warm period**.	Warmer SST (15.5 °C), increased fluvial input, relative restriction in ocean–Ría exchange. **Warm and humid period.**	(Álvarez et al., 2005; Desprat et al., 2003; Diz et al., 2002)
Ría de Muros cores	42°45′N; 8°59′W; 33–37 m bsl	Shallow marine	No data	Warmer water temperature (more negative $\delta^{18}O$). Increased freshwater discharge (fluvial regime, characterized by local productivity and retention of organic carbon). **Humid period**	(Lebreiro et al., 2006)
Almenara de Adaja	41°11′N; 4°40′W; 784 m asl	Shallow lake	Increase in the arboreal component and in Cyperaceae percentages, indicating a **warm and humid period.**	No data	(López-Merino et al., 2009)
Arreo Lake	42°46′N, 2°59′W; 655 m asl	Lake	Increased juniper component, and decreased mixed oak formations and higrophytes (mainly *Typha*), suggesting **drier conditions** than previously and during the LIA. Herbaceous component is dominant.	Warmer water temperatures (increase in *Botryococcus*), shallow lake levels and increased salinity (decrease in *Cyclotella distingüenda*, higher Sr content, gypsum precipitation). **Warm and dry period.**	(Corella, in preparation)
Basa de la Mora	42°33′N; 0°20′W; 1914 m asl	Lake	Increased *Juniperus* component, decreased *Betula* and *Corylus*, and disappearance of *Abies* as a consequence of more **dry conditions.** Significant increase in *Artemisia* (aridity indicator). For the aquatics, a decrease in the *Myriophyllum* component and disappearance of *Potamogeton*, probably because of a decline in the lake level.	Rare runoff events, indicating lower precipitation, and probably a low lake level. **Dry period.**	This study
Estanya Lake	42°02′N; 0°32′E; 670 m asl	Lake	Warmer and **drier conditions** with a landscape dominated by junipers, low proportions of mesophylic woody taxa, substantial occurrence of the heliophyte *Helianthemum*, and a poorly developed aquatic component.	Shallow lake levels and saline conditions (gypsum precipitation, low diatom abundances and presence of *Campylodiscus clypeus* fragments) with poor development of littoral environments. **Warm and dry period.**	(Morellón et al., 2011)
Montcortès Lake	42°19′N, 0°59′E, 1027 m asl	Lake	Presence of low Mediterranean scrub communities, decrease in the arboreal pollen content (mainly conifers and mesophytes), and an increase in *Artemisia* between 1100 and 1350 AD, indicating human activities as well as **warming and aridity**.	High turbidite frequency and the highest sedimentation rate in the entire sequence, as a result of the combination of climatic factors (increase in high intensity storm events, relatively lower lake levels, development of littoral environments) and changes in land use (deforestation and farming), resulting in an increase in runoff and deposition of clastic material as turbidites.	(Corella et al., 2011; Rull et al., 2011; Scussolini et al., 2011)
Central Iberia					
Tagus prodelta cores	38°33′N; 9°21′W; 90–96 m bsl	Shallow marine	No data	Higher SST and salinity (based on alkenones and isotopes), lower fluvial input (e.g. less Fe), increased upwelling (*C. laevigata* and upwelling-related diatom species). Oceanic regime (*vs.* fluvial regime in the LIA). **Warm and dry period.**	(Abrantes et al., 2005; Lebreiro et al., 2006; Rodrigues et al., 2009)

Table 1 (*continued*)

Site	Coordinates (with altitude or bathymetry)	Lake/ Marine site	MCA signal		References
			Vegetation	Hydrology/Climate	
Tablas de Daimiel	39°7′N; 3°43′W; 616 m asl	Lake	Increase in evergreen *Quercus* and changes in the aquatic vegetation, indicating the expansion of a very productive aquatic environment with a high nutrient load. **Warmer and wetter conditions.**	No data	(Gil García et al., 2007)
Taravilla Lake	40°39′N; 1°59′W; 1100 m asl	Lake	Conifers, a few mesophytes, a substantial Mediterranean component, and an increase in heliophyte shrubs, characterizing **a warm and dry period** with fewer higrophytes.	No evidence of flood deposits in the lake, lower energy environment, with less alluvial influence (contrasting with the LIA sediments, which are characterized by abundant fining upward sequences indicating flood deposits). **Warm and dry period.**	(Moreno et al., 2008; Valero-Garcés et al., 2008)
Minorca contourite - MINMC06-2 core	40°29′N; 04°01′E; 2391 m bsl	Deep marine	No data	Surface water properties (SST, salinity) do not show a clear signal during the MCA. Proxies of deep water convection indicate **reduced deep water overturning**.	This study
Southern Iberia					
Zoñar Lake	37°29′N; 4°41′W; 300 m asl	Lake	A decrease in *Olea* and mesophytes coincident with an increase in *Pistacia*, the highest proportion of heliophytes including Chenopodiaceae, the presence of *Ruppia* rather than *Myriophyllum*, and a decrease in *Botryococcus*, suggesting lower lake levels and a **dry period.**	Development of saline to brackish environments with evaporitic facies (gypsum layers), authigenic aragonite precipitation and reworking of exposed littoral sediments as a consequence of lower lake levels. Low values of Rb/Al, Ti and Si (runoff) and high values of Sr/Al (water chemical concentration). **Dry period.**	(Martín-Puertas et al., 2010)
Algerian–Balearic basin (305G and 306G cores)	36°23′N; 1°22′W; 2512 m bsl 36°27′N; 1°11′W; 2574 m bsl	Deep marine	No data	Decreased riverine input into the basin and more persistent winds from northwest Africa. Decline in fluvial-derived elements (Mg/Al, K/Al) and an increase in the Zr/Al ratio. **Dry period**	(Nieto-Moreno et al., 2011). This study

cooling of surface waters, which mostly occurs during cold and windy winters. This water increases in density until it sinks and flows from north to south along the Valencia Trough, following a cyclonic pattern at depths of approximately 2000 m (Millot, 1999). The action of those deep water currents (reworking, sorting and transporting sediments) in the western Mediterranean is responsible for the formation of a sediment drift north of Minorca Island (Velasco et al., 1996).

3. Multi-proxy methodology

The extensive application of multi-proxy methods in paleoclimatic studies of marine and lacustrine cores from the IP and surroundings seas during the last decade, combined with the more common use of statistical techniques, has led to significant advances in the reconstruction of climate variability (Moreno et al., 2012). Integrated multi-proxy approaches to the study of climate variability are critical for disentangling the various forcings, which is essential in the generation of robust reconstructions of climatic variability. Integration of data from lacustrine and marine environments provides the opportunity to differentiate among common external forcings and local or regional variability in the recorded signals. The procedure commences with an initial core description (ICD) that includes non-destructive measurement of physical properties (usually carried out using a Geotek multi-sensor core logger, which provides data on a number of parameters including magnetic susceptibility and bulk density). This is followed by the splitting of cores into halves for archiving and sampling of core sections, respectively. The identification of sedimentary structures and components using macroscopic and microscopic observations (Schnurrenberger et al., 2001) is a key step in the identification and characterization of facies. Although this protocol is particularly essential for lake sediments (Valero-Garcés et al., 2003), detailed sedimentological descriptions of marine cores also provide useful information about sedimentary processes (Lebreiro et al., 2009).

A number of geological proxies are used to help identify and characterize sedimentary processes controlling the input, transport and deposition of sedimentary particles. Such information is essential for understanding the infilling of lacustrine systems and variations between fluvial and eolian inputs to marine basins. The most commonly used proxies are: (1) the grain size distribution of total and non-carbonate particles, obtained using systems based on laser diffraction (e.g. Coulter, Malvern) or settling velocity (Sedigraph); (2) the mineralogical composition, derived from X-ray diffraction analyses; (3) elemental geochemistry, obtained at high resolution by X-ray fluorescence (XRF) core scanning (Last and Smol, 2001), or as discrete samples by other methods (e.g. inductively

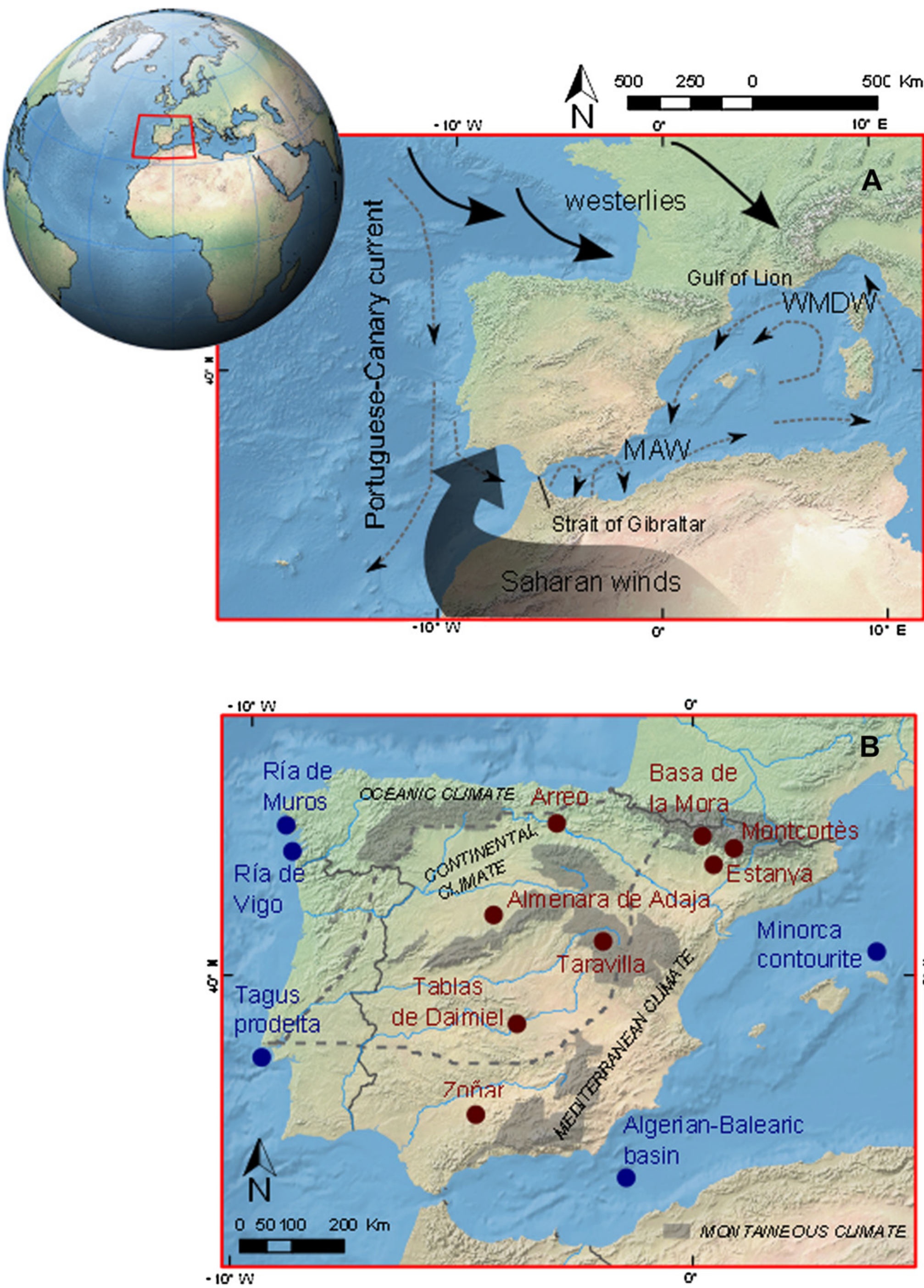

Fig. 1. (A) Oceanographic and atmospheric schematic configuration of the IP and adjacent seas. MAW: Modified Atlantic Water; WMDW: Western Mediterranean Deep Water. Black arrows represent the main wind trajectories, whereas grey dotted arrows indicate local ocean circulation patterns. (B) Map of the Iberian Peninsula showing the location of the marine (blue dots) and terrestrial (brown dots) sites involved in the study (see also Table 1). The dashed grey lines and shaded areas separate the various present-day climates (oceanic, Mediterranean, continental and mountainous). (For interpretation of the references to colour in this figure legend, the reader is referred to the web version of this article.)

coupled plasma mass spectrometry or conventional XRF); (4) the concentration of total organic carbon (TOC) and total inorganic carbon (TIC); and (5) the stable isotope composition (δ^{18}O and δ^{13}C) of carbonates, particularly in the planktonic and benthic foraminifera (marine records), or in the endogenic carbonates (lake sequences). Combined analysis of these proxies provides important information regarding, for example, the input and composition of detrital minerals in a lake *vs*. precipitated endogenic components (Corella et al., 2011), or data on the hydrological balance and temperature of lake water (Morellón et al., 2009). In the marine realm the information is related to the climatic conditions in the source areas, for example the dominance of eolian *vs*. fluvial supply (Moreno et al., 2002). In addition, common processes that can be reconstructed include variations in paleoproductivity, redox conditions (Jiménez-Espejo et al., 2007) or the intensity of paleocurrents (Frigola et al., 2007).

The most commonly used biological proxies among those available for paleoclimate reconstructions from marine and lake records are: (1) pollen and spores, which represent the types and extension of vegetation cover on land (e.g. Moore et al., 1991); (2) diatoms, ostracods and/or chironomids, which are lake organisms that provide information on environmental (temperature, precipitation) and limnological (pH, lake level, nutrients, water column mixing) conditions in lakes (e.g. Smol et al., 2001a,b); and (3) foraminifera, marine diatoms, dinoflagellates and coccolithophorids, which are marine organisms whose associations provide data about water temperature at various depths, nutrient and oxygen availability, and additional environmental information (e.g. Fisher and Wefer, 1999).

The chronology in the selected cores was primarily based on AMS ^{14}C dating of terrestrial plant remains (lake sediments) and foraminifera (marine sequences), and the dates were calibrated for this review using INTCAL09 and MARINE09 calibration curves, respectively (Reimer et al., 2009) (see Table 2 for unpublished data). Final construction of the age models was carried out by linear interpolation among the obtained dates or following the Heegaard method (Heegaard et al., 2005). For some lake sediments the chronologies were complemented using varve analysis, and $^{137}Cs/^{210}Pb$ analysis for the uppermost part of some marine and lacustrine sequences. More details about the chronological frameworks used are provided in a number of previous reports (Table 1).

4. Results

4.1. La Basa de la Mora: a record of runoff events and vegetation cover in the Central Pyrenees

La Basa de la Mora is a lake of glacial origin located at 1914 m asl in the Cotiella massif, in the Central Pyrenees (Fig. 1, Table 1). A frontal moraine on the southeastern border of the lake acts as a natural dam. Cretaceous limestones dominate the catchment area, but the bottom of the lake is sealed by impermeable fine-grained Triassic formations. Although the lake is shallow (2–3 m deep) it has a surface area of 6 ha and a permanent water lamina. The main input of water and detrital sediments comes from several creeks, which are particularly active during the annual snowmelt period. There is a small outlet from the lake in the southern part. The vegetation surrounding the lake is composed mainly of alpine grassland and *Pinus uncinata* forest. The local vegetation is diverse, varying from *Quercus ilex*–*Quercus faginea* formations on southern slopes to mixed forest of *Pinus sylvestris* and deciduous species including *Betula alba*, *Corylus avellana*, *Fagus sylvatica*, *Quercus petraea* and others on northern slopes.

The studied sequence was derived from the combination of a short gravity core, and the uppermost 2 m of a sediment core of 12 m length, which was obtained from the distal area of the lake using a UWITEC platform of the Pyrenean Institute of Ecology (IPE-CSIC) (Figs 2 and 3). For this sequence the age model was constructed using three AMS ^{14}C dates (Table 2) and the date of the ^{137}Cs peak (1963 AD at 20 cm depth). The methods used included visual description, analysis of physical properties, the geochemical composition (XRF core scanner) measured at 0.5 cm resolution, the organic and inorganic carbon content at 2 cm intervals, and analysis of pollen and spores preserved in the sediment (5–10 cm intervals). Three facies were identified based on: (1) the content of allochthonous material (inferred from MS values and percentages of siliciclastic particles) *vs*. authigenic carbonates; and (2) the type and content of organic matter. Thus, Facies 1 and 2, which were characterized by high MS values and levels of Si, Fe, K and terrestrial organic matter, appear usually associated, indicating sediment input from the catchment following episodes of intense rainfall (Fig. 2). Facies 3 represented a low energy environment, with carbonate formation over a large palustrine area probably related to low water levels. The record was divided into three units (Fig. 2) including (from bottom to top): i) Unit 3 (1–900 AD), which was characterized by high values of the siliciclastic component (Si, Fe, K; subunit 3b) that progressively decreased after 500 AD (subunit 3a); ii) Unit 2 (900–1300 AD), which was composed of carbonate sediments that contained the lowest levels of Si, Fe, K and the highest levels of Ca and TIC; and iii) Unit 1 (1300–2000 AD), which was characterized by the highest values of MS, the occasional presence of hematite, and the dominance of quartz, feldspars and phyllosilicates. Unit 1 was divided into two subunits (a and b) based on the inorganic and organic carbon content; both these parameters were at higher levels in subunit 1a (1850 AD–present). Unit 2, which was synchronous with the MCA period, contained evidence of fewer episodes of intense rainfall, higher levels of organic and carbonate productivity, and possibly the lowest lake level during the last 2000 years (the lake level during the last 150 years appears to be similar).

The pollen diagram for La Basa de la Mora (Fig. 3) indicated a relatively open landscape compared with similar settings at this altitude in the Pyrenees (the arboreal pollen content was not greater than 30% if pine pollen percentages were not included). Evidence of anthropogenic activities, in terms of herbaceous and cultivated taxa, occurred from the base of the sequence. *Pinus* was the dominant arboreal taxon, constituting >35% of the total pollen content. The presence and fluctuations of other arboreal taxa (e.g. junipers or mesophytes), and aridity/anthropogenic indicators including *Artemisia*, inferred paleoenvironmental changes in the Basa de la Mora sequence. Small variations in the lake level were evident in fluctuations in aquatic taxa (e.g. *Potamogeton*).

Table 2
Radiocarbon dating of studied cores presented for the first time in this study. The cores were analyzed at the Poznan Radiocarbon Laboratory, Poland (Poz-), the National Centre for Accelerators, Spain, (CAN), and at NOSAMS/Woods Hole Oceanographic Institution, USA (OS).

Site/region	Sample/core	Lab code	Material	Comp. depth	^{14}C ages	Cal years BP (2-σ)	Cal years AD/BC (2-σ)
Basa de la Mora, Central Pyrenees	BSM08-1A-1U-1	Poz-29744	macrorrest	26	385 ± 30	426–507	1443–1524 AD
Basa de la Mora, Central Pyrenees	BSM08-1A-1U-1	Poz-35854	macrorrest	138	1335 ± 30	1231–1304	646–719 AD
Basa de la Mora, Central Pyrenees	BSM08-1A-2U-1	Poz-29745	macrorrest	196	2100 ± 30	1995–2146	196–45 BC
Algerian–Balearic basin	305G	Poz-37150	*Globigerina bulloides*	6–7	1520 ± 30	977–1163	787–973 AD
Algerian–Balearic basin	305G	CNA567	*Globigerina bulloides*	8–9	1795 ± 40	1435–1259	515–691 AD
Algerian–Balearic basin	305G	CNA304	*Globigerina bulloides*	19–20	2320 ± 45	2063–1817	114 BC–133 AD
Algerian–Balearic basin	306G	Poz-37152	*Globigerina bulloides*	6–7	1130 ± 35	627–754	1196–1323 AD
Algerian–Balearic basin	306G	CNA306	*Globigerina bulloides*	9–10	1610 ± 45	1266–1059	684–891AD
Algerian–Balearic basin	306G	CNA307	*Globigerina bulloides*	19–20	2200 ± 60	1944–1632	6–318 AD
Minorcacontourite	MINMC-2	OS-67291	*Globigerina inflata*	11.5	845 ± 35	352–510	1440–1598 AD
Minorca contourite	MINMC-2	OS-67297	*G. inflata*	18.5	1190 ± 35	638–780	1170–1312 AD
Minorca contourite	MINMC-2	OS-67324	*G. inflata*	25.5	1540 ± 25	961–1146	804–989 AD
Minorca contourite	MINMC-2	OS-67323	*G. inflata*	29	1840 ± 30	1270–1430	520–680 AD
Minorca contourite	MINMC-1	OS-67294	*G. inflata*	7.5	895 ± 35	421–539	1411–1529 AD
Minorca contourite	MINMC-1	OS-67296	*G. inflata*	19.5	2010 ± 35	1406–1646	304–544 AD

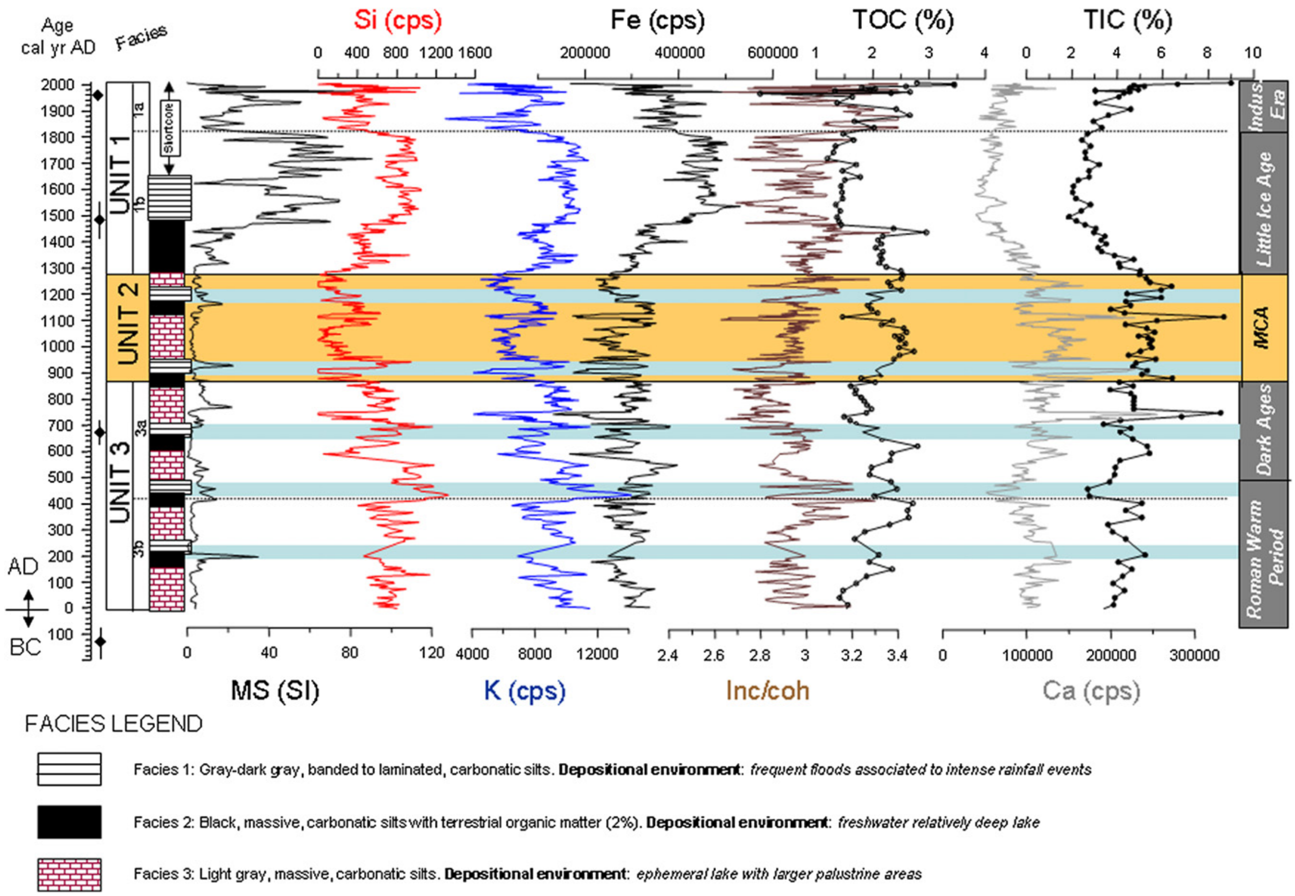

Fig. 2. The Basa de la Mora record as a function of age for the past 2000 years, including profiles of magnetic susceptibility (MS); geochemical elements measured using a XRF core scanner (Si, K, Fe, Ca, incoherence/coherence ratio) in counts per second (cps), and the percentages of total organic carbon (TOC) and total inorganic carbon (TIC). Sedimentary facies and units are indicated (see the facies legend), together with dates and the associated 2σ errors. MCA: Medieval Climate Anomaly.

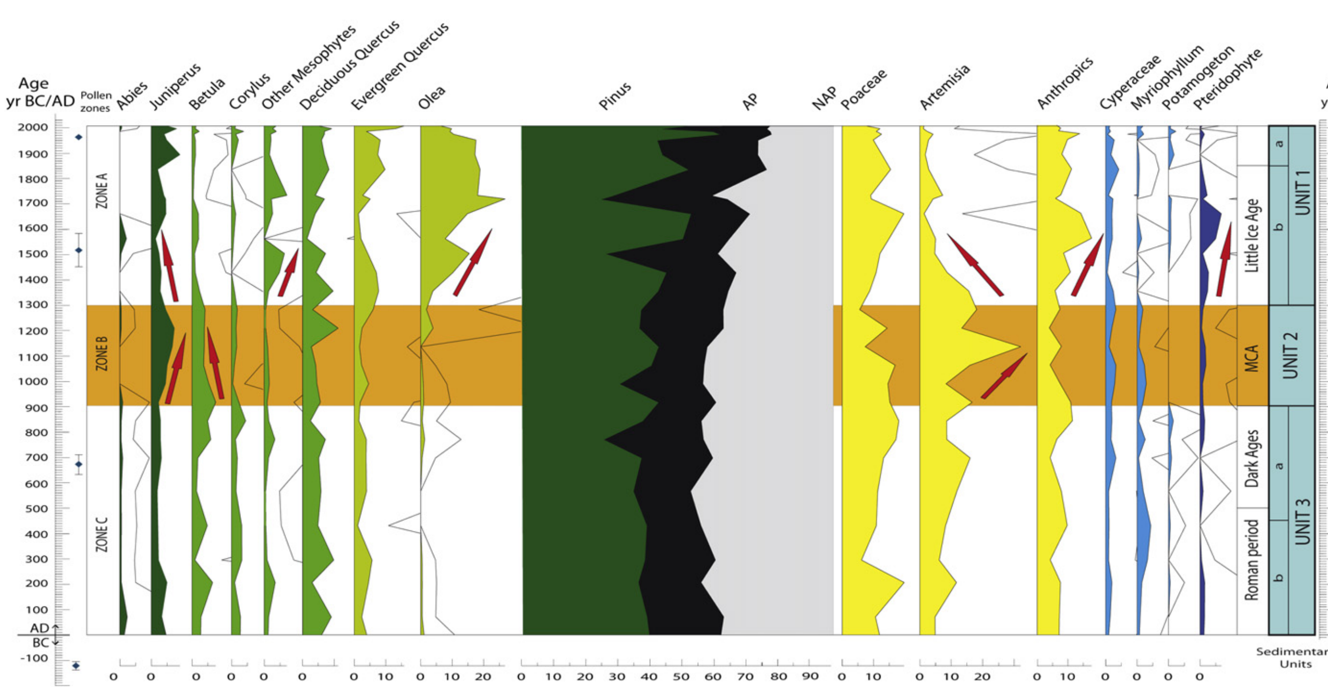

Fig. 3. Selected pollen taxa in the Basa de la Mora sequence (BSM08-1A). The 'Other Mesophytes' curve includes *Alnus*, *Carpinus*, *Salix*, *Ulmus*, *Populus*, *Fraxinus* and *Juglans*. The 'Anthropics' curve includes Cichorioideae, Carduae, Asteroideae, *Centaurea*, Caryophyllaceae, *Plantago*, *Rumex*, Brassicaceae, Urticaceae, Geraniaceae and Malvaceae. Dates and associated 2σ errors are shown. MCA: Medieval Climate Anomaly.

The pollen diagram was divided into three zones (A–C) corresponding to the sedimentary units (Figs 2 and 3). Pollen Zone C (1–900 AD) encompassed the end of the Roman Period and the Dark Ages, and recorded an open mixed forest dominated by conifers but with a significant component of *Betula*, *Corylus*, *Fagus*, deciduous *Quercus* and other mesophytes (Fig. 3). The presence of pollen of *Olea* and *Cerealia* species indicates that cultivated land was present in nearby areas. The herbaceous component (30–40%) indicated extensive pastures in high altitude mountain areas and around the lacustrine basin.

Pollen Zone B (900–1300 AD) coincided with the MCA, and recorded a considerable increase in the percentage occurrence of *Juniperus*, which reached a maximum at approximately 1200 AD. In contrast, the percentage occurrence of *Betula*, *Corylus* and deciduous *Quercus* decreased, as did the percentages of other mesophytes including *Alnus*, *Carpinus*, *Salix*, *Ulmus*, *Populus*, *Fraxinus* and *Juglans*. Coinciding with this mesophyte minimum, *Abies* disappeared from the record and *Artemisia* reached its highest percentages (up to 30%). Although there was little variation in the percentages of aquatic plants in the sequence, the absence of *Potamogeton* in this zone was the most significant change. Despite the occurrence of regional human pressure in the landscape, all these features are consistent with drier climatic conditions and a lower lake level.

Pollen Zone A (1300–2000 AD) corresponded with the LIA and the present Industrial Era, and despite ongoing trends of decrease in the occurrence of *Betula* and *Corylus*, the occurrence of members of the 'other Mesophytes' group underwent a substantial increase while the percentages of *Juniperus* and *Artemisia* decreased markedly. These features, together with the increase in Pteridophytes, the reappearance of *Abies* (which reached its maximum occurrence in this part of the sequence), and the presence of *Potamogeton*, all suggest more humid conditions, particularly for the LIA period (subunit 1b). The presence or absence of *Potamogeton* is important for the hydrological reconstruction, as this taxon requires a higher water level than does *Myriophyllum* (Bornette and Puijalon, 2011), and occupies a deeper habitat within the lake. The widespread occurrence of *Olea* and the high values of ruderal components related to pastoral activities (anthropics in the diagram in Fig. 3), evident around 1400 AD, are associated with the known expansion of human activities in the area. The vegetation changes apparent in this zone provide evidence for trends to more humid climatic conditions (deciduous *Quercus* and other mesophytes) and greater human pressure in the landscape. Analysis of the top of this zone (which coincides with the Industrial Era; subunit 1a) suggested a reversal of these trends.

4.2. MINMC06-1 and MINMC06-2 cores: a record of deep and surface water conditions off the Balearic Islands

In the northwestern Mediterranean Sea the Balearic Promontory influences the circulation of the dense WMDW formed in the Gulf of Lion, acting as a topographic barrier and changing the direction and intensity of the current. This leads to the formation off Minorca of the Minorca peripheral depression and associated sediment drift (Velasco et al., 1996), from where the IMAGES core MD99-2343 was recovered (Frigola et al., 2007, 2008). To achieve greater resolution for the last two millennia, multicores MINMC06-1 and MINMC06-2 (31 cm and 32.5 cm, respectively) were obtained at the same location as that from which the piston core MD99-2343 was recovered (Fig. 1). Grain size for the total and de-carbonated fractions, oxygen isotopes and Mg/Ca ratio on *Globigerina bulloides* and molecular biomarkers (long-chain alkenones) analyses were performed at 0.5 cm resolution. Sea surface temperature (SST) were reconstructed from (1) the relative composition of C_{37} unsaturated alkenones throughout the $U^{k'}_{37}$ index calibrated using the equation of Müller et al. (1998) and (2) the Mg/Ca ratio measured in the planktonic foraminifera *G. bulloides*. Mg/Ca is widely used as a proxy for SST (Barker et al., 2005). The Mg/Ca cleaning protocol (Pena et al., 2005) was performed without the so-called 'reductive step', and the Mg/Ca ratios were transferred to temperature using the calibration of Elderfield and Ganssen (2000). The procedures and equipment used for the analysis of C_{37} alkenones are described elsewhere (Villanueva et al., 1997).

The chronology of both multicores was based on six AMS ^{14}C dates for monospecific foraminiferan samples (Table 2), and was further refined by the comparison of the two Mg/Ca-derived SST records, which were always inside the error range provided by the dates (see dating symbols in Fig. 4). Hence, multicore MINMC06-1 covered the past 2000 years while multicore MINMC06-2 covered the past 1600 years, achieving a time resolution of 25 and 30 years, respectively. The mean sedimentation rates were 19 and 23 cm ka^{-1}, respectively, which is in the same order as that observed (24 cm ka^{-1}) at the top of the neighbouring core MD99-2343 (Frigola et al., 2007).

At this site offshore Minorca, increases in the proportion of sediment coarser than 10 μm (UP10) are related to sweeping of the sea floor by strong deep water currents that result from increased overturning in the Gulf of Lion area. This occurs because of intensification of northerly winds that cool and evaporate surface waters, which subsequently sink (Frigola et al., 2007). The UP10 records from the two multicores produced consistent results for the past 2000 years, with differences in the absolute values probably related to local differences in the setting (e.g. channel-like *vs*. lobe-like locations) (Fig. 4). The relatively high values during the last part of the Roman Period and the Dark Ages (200–900 AD), and during the first phase of the LIA (1250–1650 AD) suggest the presence of an active overturning system involving deep water formation in the Gulf of Lion. However, a decrease in the UP10 fraction during the 900–1250 AD period in each multicore suggests a major reduction in intensity of deep water currents during the MCA (Fig. 4d).

The SST values for the studied interval were consistent for both cores, marking a clear cooling trend in the last 2000 years, as has been observed in other world regions (Kaufman et al., 2009). Both methods differ in the absolute temperature values (average 20 ± 2 °C for the Mg/Ca and 15 ± 1 °C for the alkenones), although they are very similar in the reconstructed tendencies (Fig. 4b and c). Mg/Ca measured on *G. bulloides* is expected to capture the upwelling spring signal, when this foraminifer thrives as indicated in sediment trap studies (Bárcena et al., 2004), while SSTs based on alkenones represent averaged temperatures although biased towards the coldest months due the oligotrophic character of the Mediterranean in summer.

Both reconstructions signal the Roman period as the warmest period from the last 2000 years although the MCA still appears warmer than the LIA (Fig. 4). Singularly, a rather complex pattern was evident in the MCA, with an early period (900–1100 AD) of relatively lower Mg/Ca temperatures (approximately 18.5 °C) and more unstable SST-$U^{k'}_{37}$ and a later period (1100–1300 AD) of relatively warmer Mg/Ca temperatures (approximately 20 °C) with more stable SST-$U^{k'}_{37}$. The regional SST reflect here a mixture of the temperature signal in the inflowing Atlantic Ocean surface water mass with the typical climatic conditions of the Mediterranean region. Thus, it is not necessary reflecting atmospheric temperature changes over the IP since it averages the thermal signal of a wider climatic region. The Mg/Ca temperature record has been used to extract the temperature effect of the $\delta^{18}O$ from *G. bulloides* to obtain the sea water $\delta^{18}O$ ($\delta^{18}O_{sw}$), which is associated with salinity and thus becomes a proxy for sea surface salinity (SSS). The results show a relatively constant SSS throughout the study period, with the relative absence of oscillations indicating that the period prior to the MCA (the Roman Period and Dark Ages) was dominated by

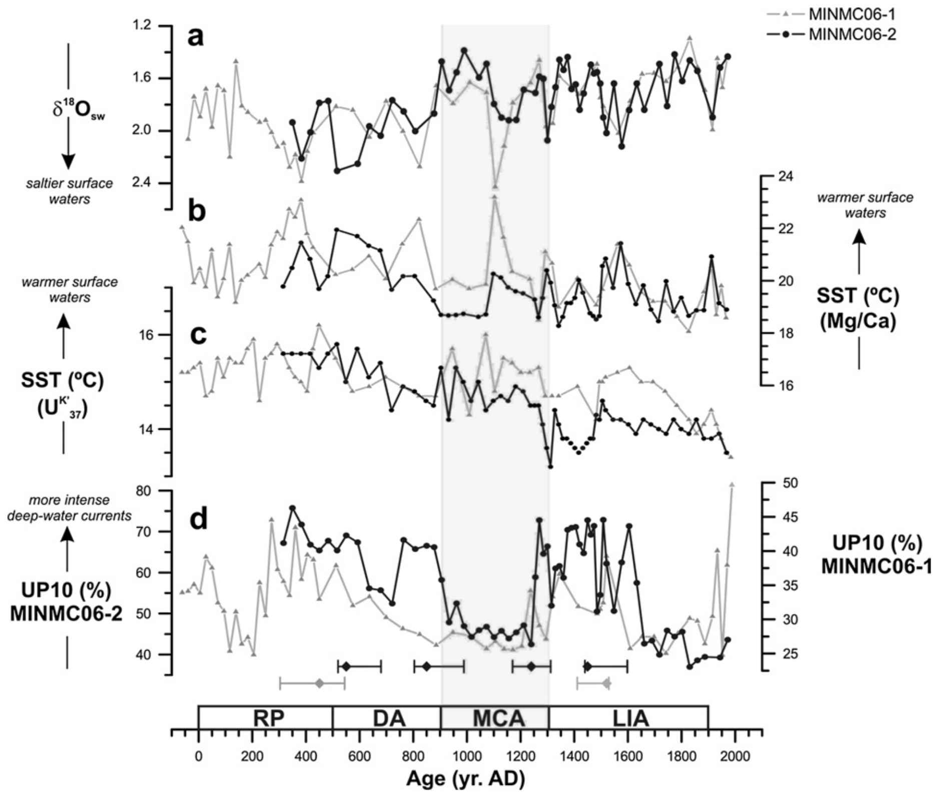

Fig. 4. Minorca short core (MINMC06-1 and MINMC06-2) profiles as a function of age for the past 2000 years. From top to bottom: (a) the $\delta^{18}O_{sw}$ record indicates the salinity of surface waters; the sea surface temperature (SST) profile derived from (b) the Mg/Ca ratio and (c) the $U^{k'}_{37}$ index, as indicators of temperature; and (d) the percentage of the fraction coarser than 10 μm (UP10 fraction), as an indicator of deep water current intensity. The dates and associated 2σ errors for each core are indicated at the bottom. RP: Roman Period; DA: Dark Ages; MCA: Medieval Climate Anomaly; LIA: Little Ice Age.

highly saline sea surface waters (Fig. 4a). Within the MCA the SSS record also differentiates two periods, with more saline waters during the latter period (1100–1300 years AD), although the salinity was not significantly higher than in other subsequent periods during the LIA.

Thus, the records of surface water properties (SST and salinity) did not differentiate the MCA, but proxies of deep water convection showed a very distinctive signature for this period, particularly reduced deep water overturning. These changes were associated with climate patterns in the area of deep convection (the Gulf of Lion), and were probably associated with more stable atmospheric conditions and less intense winds, which were unable to disrupt the well stratified water column and resulted in reduced intensity of deep water currents (Fig. 4d).

4.3. Algerian–Balearic basin cores: detrital input and climate response

The climate signal for the last two millennia was reconstructed using two marine cores (305G, 306G) from the west Algerian–Balearic basin (Fig. 1, Table 1), which were recovered during the Training Trough Research 14 (R/V Professor Logachev) oceanographic cruise. The lithology of these sediments mainly consisted of homogeneous green–brown hemipelagic muds–clays in the upper part, which became darker with increasing depth and contained foraminifera and shell fragments (Comas and Ivanov, 2006). The content of major elements and zirconium (Zr) was measured at 1 cm intervals using wavelength dispersive X-ray fluorescence spectrometry.

The age–depth models for the study time period were based on six AMS ^{14}C dates complemented with the activity–depth profiles of ^{210}Pb in the top 5 cm in each core (core lengths of 40 cm and 35 cm for cores 305G and 306G, respectively) (Nieto-Moreno et al., 2011) (Table 2). The results showed that ^{210}Pb was in excess only in the top 2 cm (Nieto-Moreno et al., 2011). Linear interpolation was applied between the ^{14}C dates, yielding mean sedimentation rates of 10.2 and 10.7 cm ka^{-1} for cores 305G and 306G, respectively. The mean sedimentation rates and ^{210}Pb inventories were similar to those previously reported for other deep Mediterranean areas (Garcia-Orellana et al., 2009), but lower than for other sediment records for the area (Masquè et al., 2003), suggesting a possible loss of the surface sediment during the gravity core recovery. The enrichment of ^{210}Pb in the first centimeters of each core suggests that the loss of sediment was not significant, which is consistent with the age model inferred from the ^{14}C-AMS dates (Nieto-Moreno et al., 2011). In previous studies of the region selected elemental ratios (Zr/Al, Mg/Al and K/Al) have been used to infer fluctuations in terrestrial runoff, erosional processes, and riverine and eolian input to the Algerian–Balearic basin (Moreno et al., 2005; Jiménez-Espejo et al., 2007, 2008; Rodrigo-Gámiz et al., 2011). Aluminium normalization is commonly used to identify fluctuations in detrital alumino-silicate source materials (e.g. van der Weijden, 2002).

Interpretation of the geochemical changes reflected in each of the cores from southern Iberia indicated a marked trend of increase in fluvial-derived elements (Mg/Al and K/Al). This occurred during the latter part of the Roman Period, peaked at the end of this period, then progressively decreased until the LIA (Fig. 5). Thus, the greatest fluvial input into the Algerian–Balearic basin occurred during the RP, which was by far the most humid period during the past 2000 years in the western Mediterranean (Martín-Puertas et al., 2008, 2010; Nieto-Moreno et al., 2011). A progressive decrease from the beginning of the DA until the middle LIA reflects a progressive

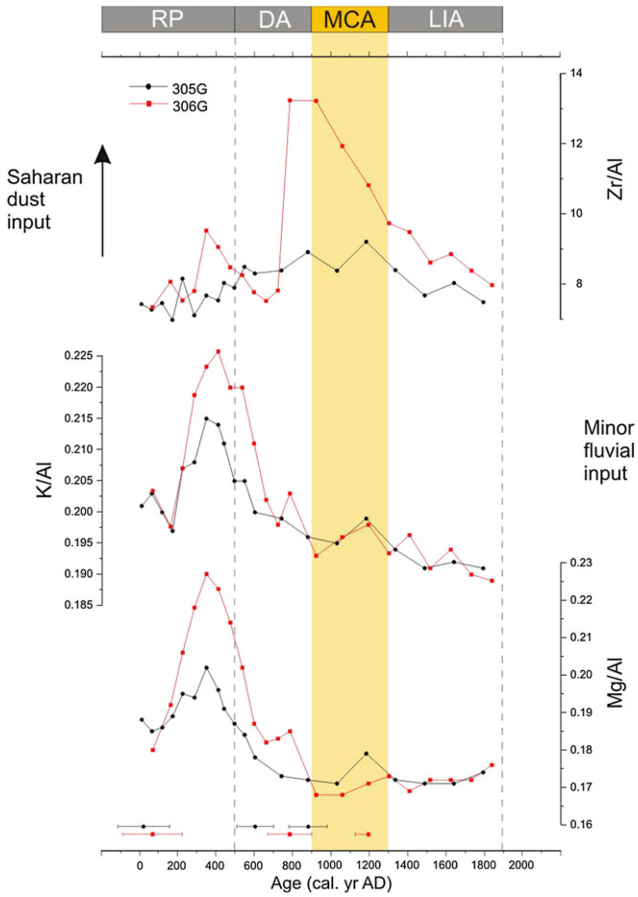

Fig. 5. Algerian–Balearic basin records (305G, black circles; 306G, red squares cores) as a function of age for the past 2000 years. From top to bottom, the Zr/Al ratio is a proxy for Saharan dust input, and the K/Al and Mg/Al ratios represent fluvial input. The dates and associated 2σ errors for the two cores are indicated at the bottom. RP: Roman Period; DA: Dark Ages; MCA: Medieval Climate Anomaly; LIA: Little Ice Age. (For interpretation of the references to colour in this figure legend, the reader is referred to the web version of this article.)

decline of riverine input during the study period. The Zr/Al ratio, which is associated with changes in Saharan eolian input, showed a consistent pattern, with the highest values occurring at the end of the DA and during the early MCA, and the lowest values occurring in the early RP and the LIA. This suggests drier conditions, more persistent northwest African winds, and thus higher eolian input into the Algerian–Balearic basin during the MCA.

5. Paleohydrological signal during the MCA: a compilation of Iberian marine and terrestrial records

Most of the multi-proxy reconstructions considered in this study indicated relatively arid conditions (represented by shallower lake levels, dominance of arid-adapted vegetation, and greater inputs of Saharan dust) during the MCA relative to the LIA. Fig. 6 shows representative Iberian records, and Fig. 7 shows the main pollen taxa found in various lacustrine records from the IP.

5.1. The northeast: from the Pyrenees to the Balearic basin

5.1.1. Lake and marine records: Basa de la Mora, Estanya, Arreo, Minorca contourite

The cores from La Basa de la Mora constitute the most complete high altitude record available for the past two millennia in the Pyrenees. Both the geochemical composition of the sediment and the vegetation cover in the catchment indicate a lower lake level and a drier environment during the DA and the MCA (Fig. 6F). The record from Arreo Lake (northwestern Ebro Basin; Fig. 1) shows a clear increase in the Sr content of endogenic carbonates, which is interpreted as reflecting higher water salinities and lower lake levels during the MCA (Corella, in preparation) (Fig. 6C). The reconstruction for Estanya Lake (Pre-Pyrenees), which was largely based on sedimentary facies and elemental and isotopic geochemistry, clearly identified an increase in the lake level from the end of the MCA to the LIA (Morellón et al., 2011). Fig. 6D shows the reconstructed salinity for Estanya Lake, which was based on principal component analysis of the elemental and geochemical dataset (Morellón et al., 2009, 2011, 2012).

From a palynological point of view (Fig. 7 and Table 1), several indicators suggest a drier MCA in northeastern Iberia. These include: i) the predominance of sclerophyllous Mediterranean vegetation, including an increase in the presence of *Juniperus* in La Basa de la Mora and Estanya lakes (Morellón et al., 2011) and evergreen *Quercus* in Montcortés Lake (Rull et al., 2011); ii) the occurrence of fewer deciduous trees in a landscape (e.g. Arreo, Basa de la Mora, Estanya, Taravilla) with a generally reduced arboreal component (Corella, in preparation; Moreno et al., 2008; Morellón et al., 2011; Pérez-Sanz et al., 2011, respectively); iii) the presence and/or increase of heliophytes in areas including Basa de la Mora, Montcortés and Taravilla (Moreno et al., 2008; Rull et al., 2011); and iv) changes in the aquatic component, including a decrease in or the disappearance of some hydrophytes (e.g. *Potamogeton*) in La Basa de la Mora (Fig. 3).

Thus, in general terms, arid conditions in the continent are indicated by higher water salinity and/or low lake levels, and changes in the regional vegetation. The marine data highlights an episode of stronger deep water formation after 1300 AD, corresponding to the LIA (Fig. 4c). Interpreted in the same way as for the entire Holocene record (Frigola et al., 2007), the former result points to a weaker influence of westerly winds during the MCA, with dry and cold winds having been responsible for deep water formation in the Gulf of Lion.

5.1.2. Cultural vs. climatic landscapes: Montcortès and Taravilla lakes

Other northeastern Iberian palynological sequences that have been used to reconstruct landscapes for the MCA period have also indicated the occurrence of arid conditions. However, most are interpreted as “cultural landscapes” (Miras et al., 2007; Pèlachs et al., 2009; Ejarque et al., 2010) that are the result of human activities and not the consequence of warmer and/or drier climatic conditions. Although anthropogenic activities in the IP have been significant since Neolithic times (Barandiarán et al., 2007), the paleoenvironmental history of the past 2000 years is a product of the interplay between climate change and human activities, making it difficult to discern and evaluate the roles of each in the absence of a multi-proxy study.

The sedimentary sequence from Montcortès Lake (Pre-Pyrenees) reflects the interaction between climatic and human influences. Thus, as described above for other northeastern records, the thermophilous plant associations during the MCA are indicative of a warm climate (Rull et al., 2011), and are consistent with the changes in *Pseudoschizaea* associated with erosion processes, drier conditions, and probably lower lake levels. In addition, between 710 and 1300 AD diatoms were poorly preserved, or possibly rare or absent because of low lake levels and alkaline water conditions (Scussolini et al., 2011). However, sedimentological and geochemical indicators suggest an increase in human activities in the lake watershed under the favourable climatic conditions that existed in mid-mountain areas during the MCA. Fig. 6G shows the number of

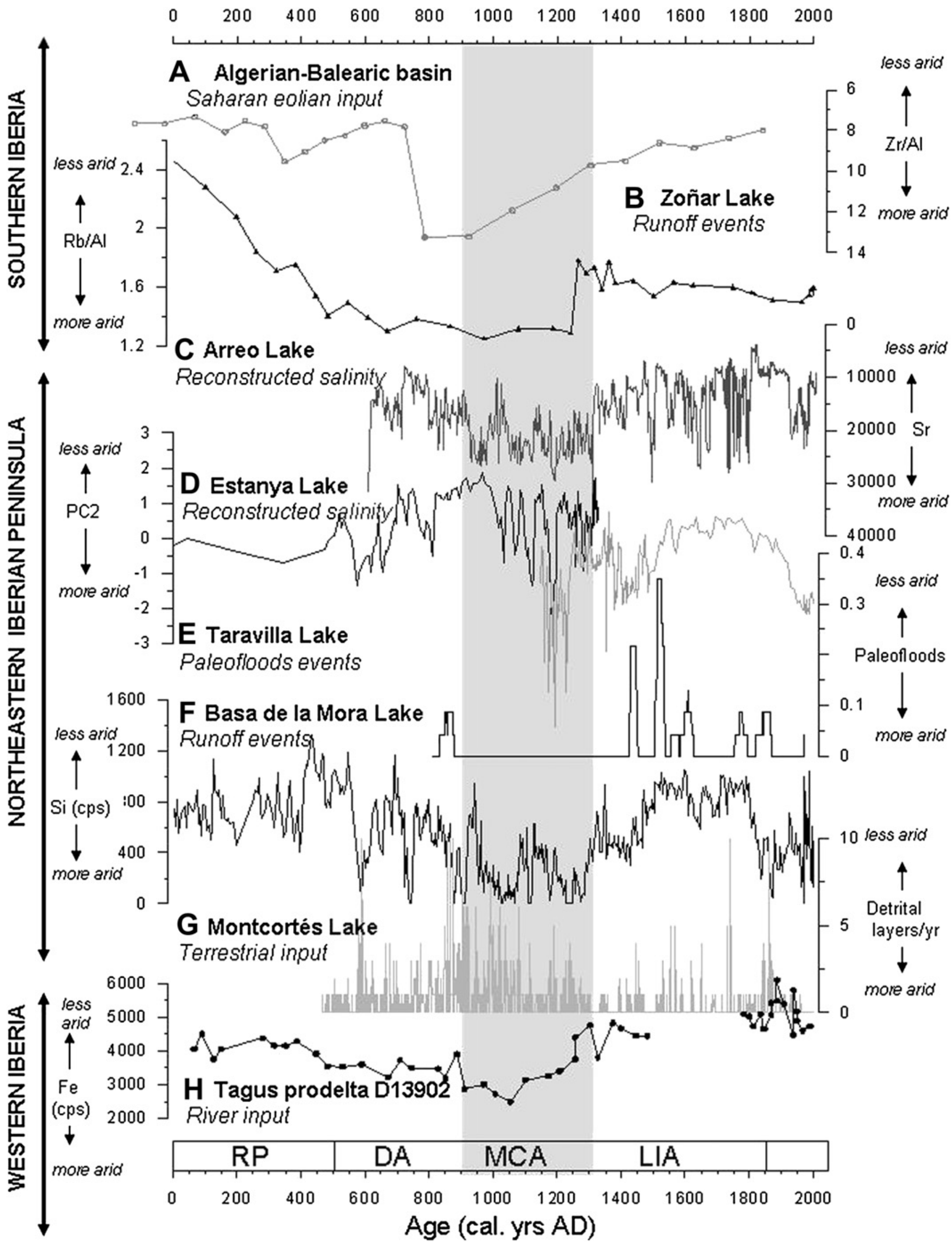

Fig. 6. Selected records from Central and Mediterranean Iberia covering last 2000 years that indicate variations in aridity. From top to bottom: A) Zr/Al ratio from Algerian–Balearic basin core; B) Rb/Al ratio from Zoñar Lake; C) Sr (cps) from Arreo Lake; D) the aridity reconstruction of Estanya Lake (axis 2 from the Principal Component Analyses applied to the XRF dataset in two cores); E) the number of paleoflood events in Taravilla Lake; F) Si (cps) from Basa de la Mora Lake; G) the number of detrital layers per year from Montcortès Lake and H) Fe (cps) from the Tagus prodelta. Note that all records are plotted to indicate arid conditions towards the bottom. RP: Roman Period; DA: Dark Ages; MCA: Medieval Climate Anomaly; LIA: Little Ice Age.

detrital events per year as an indicator of surface runoff in the lake catchment (Corella et al., 2011). The high frequency of turbidite layers and the occurrence of the highest sedimentation rate in the entire sequence (3.1 mm yr^{-1}) is indicative of an increase in sediment delivery to Montcortès Lake, which commenced in approximately 800 AD and continued (albeit with a general trend of decrease) during the MCA (Fig. 6G). The turbidite layers in the Montcortès Lake correspond to single events of terrigenous sediment influx transported by increased runoff from the watershed. It is very difficult to establish whether the greater sediment delivery during the MCA was the result of climatic factors (increase in storm events, relatively low lake levels because of higher temperatures, more intense evaporation and decreased precipitation, more development of littoral environments), a consequence of changes in land use practices (deforestation, farming and intensification of cultivation), or a combination of these factors. As noted above, human impact and climate variability have probably acted synergistically on the Iberian lakes and vegetation landscapes throughout history. Although increased anthropogenic activities in the watershed would have greatly increase sediment delivery to

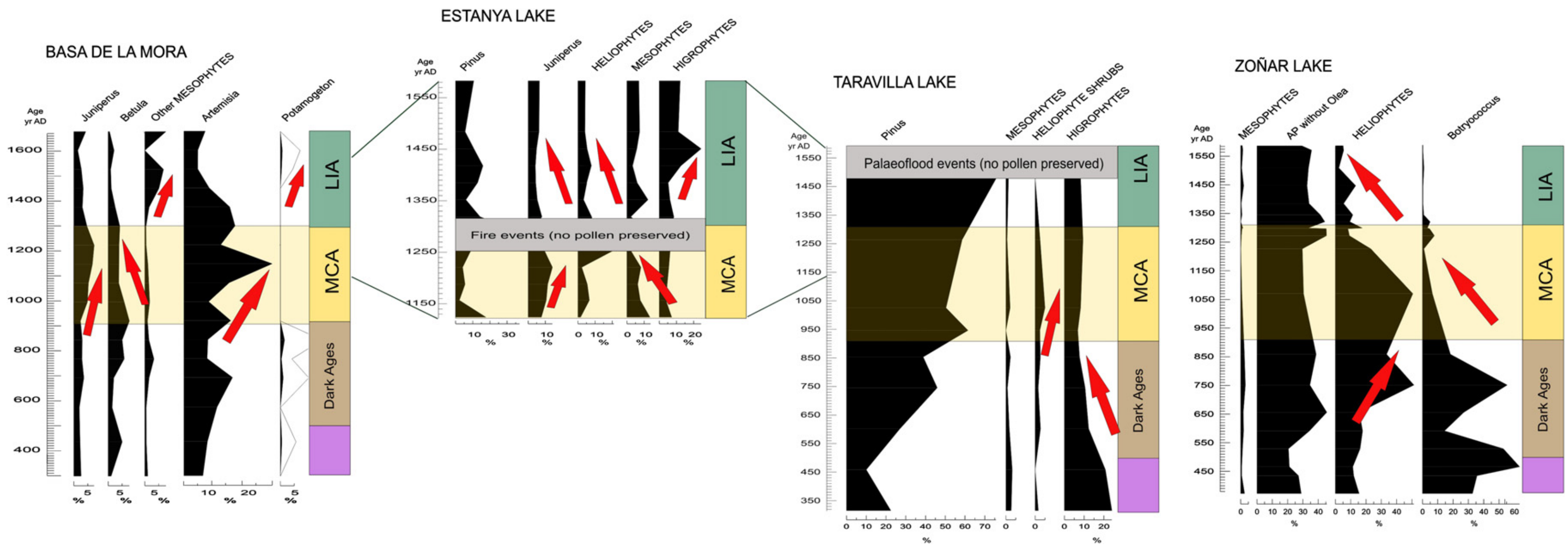

Fig. 7. Age profiles for selected pollen taxa and groups from La Basa de la Mora, Estanya, Taravilla and Zoñar lakes. The yellow band marks the MCA record, and shows a similar climatic pattern (an increase in drier conditions). In the Basa de la Mora record 'Other MESOPHYTES' includes *Alnus*, *Carpinus*, *Salix*, *Ulmus*, *Populus*, *Fraxinus* and *Juglans*. For Estanya lake, 'HELIOPHYTES' includes *Artemisia*, *Helianthemum*, Cichorioideae and Chenopodiaceae; 'MESOPHYTES' includes deciduous *Quercus*, *Betula*, *Corylus*, *Alnus*, *Tilia*, *Ulmus*, *Populus*, *Salix* and *Fagus*; and 'HIGROPHYTES' includes *Tamarix*, *Typha* and Cyperaceae. For Taravilla Lake, 'MESOPHYTES' includes deciduous *Quercus*, *Betula*, *Corylus*, *Salix*, *Ulmus*, *Populus*, *Tilia* and *Juglans*; 'HELIOPHYTE SHRUBS' includes *Ephedra fragilis*, *Thymelaea* and *Helianthemum;* and 'HIGROPHYTES' includes Cyperaceae and Typha. For Zoñar Lake 'MESOPHYTES' includes deciduous *Quercus*, *Juglans*, *Alnus*, *Populus*, *Ulmus*, *Fraxinus* and *Salix*; and 'HELIOPHYTES' includes *Ephedra fragilis*, *Ephedra dystachia*, *Artemisia*, Asteroideae, Cichorioideae, Chenopodiaceae and *Helianthemum*. (For interpretation of the references to colour in this figure legend, the reader is referred to the web version of this article.)

the lake, biological indicators (pollen and diatoms) (Rull et al., 2011; Scussolini et al., 2011) suggest that dry climatic conditions occurred during the MCA.

A clearer paleohydrological signal without evidence of human forcing is recorded in Taravilla Lake, located in the Iberian Range in the headwaters of the Tagus River (Fig. 1). Coarse grain size layers having high siliciclastic content were deposited in this lake during paleoflood events caused by increased runoff associated with intense rainfall (Moreno et al., 2008; Valero-Garcés et al., 2008). Evidence for peaks in the content of *Cerealia*, ruderal plants and other anthropogenic taxa associated with crops are present in the base of the sequence (data not shown, see Moreno et al., 2008), indicating intense human activities when terrigenous paleoflood layers are scarce while there are no evidences of human activities synchronously with the increase in terrigenous layers. Thus, significant removal of vegetation by human-caused fires or deforestation practices cannot be the main factor driving the increase in terrigenous layers (Moreno et al., 2008). Changes in the amount, frequency and intensity of precipitation have an effect on the magnitude and timing of runoff and the intensity of floods, even in small catchments including that of Taravilla Lake (Moreno et al., 2008). It is noteworthy that the paleoflood layers were thicker and more frequent during the LIA (Fig. 6E). The long-term database produced from the stratigraphic record of slack water flood deposits in the Tagus River basin (Benito et al., 2003a,b; Thorndycraft and Benito, 2006) is consistent with the Taravilla Lake dataset. Despite minor differences in the timing, both records demonstrate that the MCA was a period with few extreme events (or less intense events that are not evident in the record), while the LIA was characterized by an increase in the frequency of flood episodes (Moreno et al., 2008).

Thus, despite local differences and some dating uncertainties, the MCA in northeastern Iberia was evidently a relatively dry period characterized by weaker westerly winds, a low frequency of extreme rainfall events (flood episodes), and decreased lake water levels favouring the development of more arid-adapted vegetation.

5.2. The west and the south: from the Atlantic Ocean to the Mediterranean Sea

Three high resolution sequences were selected from the southern Iberian area, including the Zoñar Lake sequence (Martín-Puertas et al., 2010) and two sequences from the Algerian–Balearic basin (305G and 306G) (Fig. 5). The record indicates that for Zoñar Lake a reduction in detrital input (clay minerals, quartz, feldspar and detrital calcite) into the lake occurred during a period of reduced precipitation (Martín-Puertas et al., 2010). Among the numerous geochemical indicators of clastic input, the Rb/Al ratio shown in Fig. 6B was selected because of its strong correlation with the detrital component, and because it was less influenced by other in-lake processes (Martín-Puertas et al., 2010). Both the Rb/Al ratio and pollen indicators, the latter evident as an increase in heliophytes (Fig. 7) marked by a significant peak of *Chenopodiaceae* (Martín-Puertas et al., 2008), indicate a dry climate in the southern IP (see Fig. 6B) during the MCA. A similar pattern can be deduced from other palynological sequences of southern Iberia, including those from Cañada de la Cruz (Carrión et al., 2001) and Siles Lake (Carrión, 2002), which show a clear decrease in mesophytes and an increase of xerophytes indicative of regional aridity.

In the marine realm the available cores show a consistent pattern of variation. The Zr/Al ratio found in the Algerian–Balearic basin is shown in Fig. 6A, and provides a good indication of aridity, as this ratio is related to the input of Saharan dust (Jiménez-Espejo et al., 2007; Nieto-Moreno et al., 2011; Rodrigo-Gámiz et al., 2011). These profiles point to dry conditions during the MCA, with more persistent winds coming from northwest Africa and/or more arid conditions in the North African source areas.

Few high resolution terrestrial records covering this time period are available for the western IP, preventing a detailed comparison of the MCA paleohydrological signal on the Atlantic Ocean side of the IP. However, a clear increase in temperature during the MCA was reconstructed from the mercury concentrations in a Galician peatbog (Martinez-Cortizas et al., 1999). Several studies of offshore Galicia cores obtained from the Ría de Muros (Lebreiro et al., 2006; Pena et al., 2010) and the Ría de Vigo (Desprat et al., 2003; Álvarez et al., 2005), and several cores recovered from the Tagus prodelta (Rodrigues et al., 2009) suggest warmer temperatures prevailed during the MCA than during the LIA (Table 1). More importantly, an opposite pattern with respect to humidity was detected in cores from offshore Galicia (northwest) and offshore Lisbon (southwest) (Fig. 1). Thus, based on the offshore Lisbon record the MCA is characterized as a dry period, as inferred from a decrease in runoff and river-induced productivity (Abrantes et al., 2005) (Fig. 6H), while sedimentological and geochemical data from the Ría de Muros sequence (Lebreiro et al., 2006) suggest more humid conditions during the MCA. In the Ría de Vigo record warmer conditions were deduced from palynological proxies (Desprat et al., 2003), but no variations in humidity were evident. Other sequences from northwestern Spain were reviewed to explore the variations in humidity during the MCA. Thus, although based only on palynological indicators, the sequence of Almenara de Adaja (López-Merino et al., 2009) (Fig. 1, Table 1) clearly indicates an increase in humidity from 900 to 1300 AD. Similarly, the record from Tablas de Daimiel (central Spain) also indicates wetter conditions during the MCA compared with subsequent centuries (Gil García et al., 2007). Opposite hydrological conditions during the MCA are indicated in records from the northwest (Atlantic Ocean influence) relative to those from the south and northeast, where a Mediterranean influence predominated.

5.3. Climate mechanisms for the MCA signal documented in Iberian records

Most of the Iberian records discussed above indicate warm conditions during the MCA, in agreement with recent global paleoclimate reconstructions (Seager et al., 2007; Mann et al., 2009). Climate variability during the last millennium has been attributed to fluctuations in solar irradiance and tropical volcanic eruptions (e.g. Wanner et al., 2008), and the role of the NAO has recently been suggested to explain the differences in humidity among the MCA and the LIA (Trouet et al., 2009, 2012). In fact, solar irradiance and the NAO are related, as indicated by recent global climate model experiments that shown how an increase (decrease) in solar irradiance can force a shift towards a high (low) NAO index (Mann et al., 2009). A positive NAO index results in a warmer and more arid climate in the western Mediterranean region. Accordingly, less river discharge offshore from Lisbon (Lebreiro et al., 2006; Alt-Epping et al., 2009), lower lake levels in northeast (Morellón et al., 2012) and southwest Iberia (Martín-Puertas et al., 2010), less flood events in the Tagus River basin (Benito et al., 2004; Moreno et al., 2008), and major Saharan eolian input in the westernmost part of the Mediterranean Sea (Nieto-Moreno et al., 2011) have been reconstructed (Fig. 6). Westerly winds must have been shifted northwards (central and northern Europe), consistent with a positive NAO index at this latitude. Dominant positive NAO phases would have been conducive to dry climatic conditions and more xerophytic and heliophytic vegetation, as shown by the pollen records from northern to southern Iberia (Fig. 7). Recent model simulations of precipitation in the IP support the role of the NAO in creating a dry anomaly during medieval times, although there are still large uncertainties in the evolution of precipitation during the last millennium (Gómez-Navarro et al., 2010). Exceptions to the general Iberian pattern that indicate a more humid climate during the MCA are evident in some records from the northwest, including marine cores from Ría de Muros and the Almenara de Adaja peatbog (Lebreiro et al., 2006; López-Merino et al., 2009; Table 1). However, these records are consistent with the hypothesis of a dominant positive NAO during the MCA. During positive phases of the NAO the northwest region of the IP is affected by north-shifted westerly winds, which could explain the observed increase in precipitation (Fig. 1). The central region of Iberia, only represented here by the Tablas de Daimiel record (Gil García et al., 2007), can be considered to be a transitional zone in terms of humidity conditions during the MCA. However, more analyses (some currently in progress) and improved chronologies are necessary to clarify the climate mechanisms responsible for the spatial patterns of environmental change in the IP during the MCA.

Records from other areas of Europe, particularly the Mediterranean region, have been compared with the Iberian sequences to analyze the hydrological signal during the MCA. Thus, north African records including those derived from tree rings (Esper et al., 2007) and lake sediments (Détriché et al., 2009) from Morocco are consistent with the main findings for the Mediterranean Iberia, and indicate dry conditions during the MCA. Interestingly, reconstructions of temperature and precipitation during the MCA, based on pollen and lake level data from the Jura Mountains (Magny et al., 2010, 2011), indicate a correlation with positive NAO conditions. Studies of speleothems from the Alps (Mangini et al., 2005) suggested the MCA was a warm period, but no evidence of hydrological changes was presented.

The timing of the end of the MCA is not resolved at a decadal scale. Depending on the proxy and the chronology and resolution of the various records, the transition from the MCA to the LIA occurred in the vicinity of 1300–1400 AD. Despite local chronological uncertainties associated with radiometric dating, the signal suggesting a period of low temperatures and generally increased humidity is consistent in the southern–central European and Mediterranean records analyzed (e.g. Büntgen et al., 2011). The LIA was characterized in the Gulf of Lion by an increase in storminess (Dezileau et al., 2011), which may have been related to a southward shift in the storm tracks in relation to a negative phase of the NAO. Other reconstructions, based on tree rings, historical archives and climatological data, also indicate a negative (cooler) phase of the NAO for the LIA (Luterbacher et al., 2001). Thus, although the role of the NAO mode during the MCA needs further evaluation using climate models and other proxy records from the northernmost European region, the Iberian data support this hypothesis. The change in solar activity documented in the transition from the MCA to the LIA (approximately 1350 AD) seems to have influenced the general atmospheric circulation pattern in the North Atlantic (Shindell et al., 2001), and this was probably reflected in a change to a period dominated by more negative modes of the NAO.

Records from the eastern Mediterranean region show similarities in the timing of the main abrupt hydrological changes observed in the west and central Mediterranean (e.g. MCA *vs*. LIA), but with different/opposite responses (see Roberts et al., 2012). Thus, the record from the Nar crater lake in Turkey showed very positive $\delta^{18}O_{calcite}$ values indicative of dry climatic conditions from 300 to 500 AD and again from 1400 to 1960 AD, and more negative isotopic values indicative of a wetter climate in the periods 560–750 AD, 1000–1400 AD and 1960–2000 AD (Jones et al., 2006). The Dead Sea (Neumann et al., 2007), Lake Van (Wick et al., 2003) and Ioannina (Frogley et al., 2001) records also show similarities with the Nar lake sequence, with differences able to be explained in terms of the various proxies used (e.g. lake water level *vs*. lake oxygen isotopes). It appears that there is generally good agreement among the records for the period from approximately 800–1750 AD, which indicate generally wetter climatic conditions around 1200 AD (MCA) and somewhat drier conditions during most of the LIA (Roberts et al., 2012).

6. Conclusions

Selected records from the IP, including marine and terrestrial sequences, have provided a coherent paleoclimate reconstruction for the past 2000 years, largely in terms of humidity variations. Particularly for the MCA period (900–1300 AD), the selected records from Mediterranean IP generally indicate drier conditions, evidenced in the lake sediments by lower water levels and higher chemical concentrations, while in marine cores a decrease in fluvial supply and an increase in Saharan dust particles has been detected. Consistent with these results, the pollen records suggest a vegetation landscape containing high levels of xerophytic or heliophytic taxa. The records from northwest Iberia indicate that there was an increase in humidity during the MCA, thus reflecting an opposite behaviour to the Mediterranean Iberia.

The position of the IP on the southern edge of the storm tracks associated with mid-latitude westerly winds, and the marked impact of NAO dynamics on moisture availability throughout most of Iberia, enable the hypothesis of Trouet et al. (2009), that the MCA was dominated by a positive NAO index, to be tested. The reconstruction for the MCA, which suggests the presence of a warmer climate and relatively arid conditions in the Mediterranean Iberia but increased humidity on the Atlantic Ocean side of the peninsula, is consistent with a role for the NAO in having shaped the climate of the IP during the last millennium. More paleoclimatic studies, particularly in western and central regions, will improve the spatial coverage of the IP, and clarify the spatial variability of climatic fluctuations in this region.

Acknowledgements

Funding for this study was largely derived from the CALIBRE (CGL2006-13327-C04), HIDROPAST (CGL2010-16376), GLOBALKARST (CGL2009-08415), DINAMO (CGL2009-07992), HOLONED (CGL2009-07603) and GRACCIE-CONSOLIDER (CSD2007-00067) projects, provided by the Spanish Inter-Ministry Commission of Science and Technology (CICYT). A. Moreno acknowledges postdoctoral funding from the Ramón y Cajal program. We are very grateful to Susana Lebreiro, Teresa Rodrigues, Vania Stefanova, Neil Roberts and Matthew Jones for their data and discussion suggestions. Miguel Sevilla is acknowledged for his assistance with Fig. 1.

References

Abrantes, F., Lebreiro, S., Rodrigues, T., Gil, I., Bartels-Jonsdottir, H., Oliveira, P., Kissel, C., Grimalt, J.O., 2005. Shallow-marine sediment cores record climate variability and earthquake activity off Lisbon (Portugal) for the last 2000 years. Quaternary Science Reviews 24, 2477–2494.

Alt-Epping, U., Stuut, J.-B.W., Hebbeln, D., Schneider, R., 2009. Variations in sediment provenance during the past 3000 years off the Tagus River, Portugal. Marine Geology 261, 82–91.

Álvarez, M.C., Flores, J.A., Sierro, F.J., Diz, P., Francés, G., Pelejero, C., Grimalt, J.O., 2005. Millennial surface water dynamics in the Ría de Vigo during the last 3000 years as revealed by coccoliths and molecular biomarkers. Palaeogeography, Palaeoclimatology, Palaeoecology 218, 1–13.

Barandiarán, I., Martí, B., del Rincón, M.A., Maya, J.L., 2007. Prehistoria de la Península Ibérica (6ª edición actualizada). Ariel S.A., Barcelona.

Bárcena, M.A., Flores, J.A., Sierro, F.J., Pérez-Folgado, M., Fabres, J., Calafat, A., Canals, M., 2004. Planktonic response to main oceanographic changes in the Alboran Sea (Western Mediterranean) as documented in sediment traps and surface sediments. Marine Micropaleontology 53, 423.

Barker, S., Cacho, I., Benway, H., Tachikawa, K., 2005. Planktonic foraminiferal Mg/Ca as a proxy for past oceanic temperatures: a methodological overview and data compilation for the last glacial maximum. Quaternary Science Reviews 24.

Benito, G., Díez-Herrero, A., Fernández de Villalta, M., 2003a. Magnitude and frequency of flooding in the Tagus basin (Central Spain) over the last millennium. Climatic Change 58, 171–192.

Benito, G., Sopeña, A., Sánchez-Moya, Y., Machado, M.J., Pérez-González, A., 2003b. Paleoflood record of the Tagus River (Central Spain) during the late Pleistocene and Holocene. Quaternary Science Reviews 22, 1737–1756.

Benito, G., Díez-Herrero, A., Fernández de Villalta, M., 2004. Flood response to solar activity in the Tagus basin (Central Spain) over the last millennium. Climatic Change 66, 27–28.

Blanco-Castro, E., Casado, M., Costa, M., Escribano, R., García Antón, M., Génova, M., Gómez, A., Moreno, J., Morla, C., Regato, P., Sainz Ollero, H., 1997. Los bosques ibéricos. Una interpretación geobotánica. Planeta, Barcelona.

Bornette, G., Puijalon, S., 2011. Response of aquatic plants to abiotic factors: a review. Aquatic Sciences 73, 1–14.

Büntgen, U., Tegel, W., Nicolussi, K., McCormick, M., Frank, D., Trouet, V., Kaplan, J.O., Herzig, F., Heussner, K.-U., Wanner, H., Luterbacher, J.r., Esper, J., 2011. 2500 years of European climate variability and human susceptibility. Science.

Carrión, J.S., Munuera, M., Dupré, M., Andrade, A., 2001. Abrupt vegetation changes in the Segura mountains of southern Spain throughout the Holocene. Journal of Ecology 89, 783–797.

Carrión, J.S., 2002. Patterns and processes of Late Quaternary environmental change in a montane region of southwestern Europe. Quaternary Science Reviews 21, 2047–2066.

Comas, M.C., Ivanov, M.K., 2006. Eastern Alboran margin: the transition between the Alboran and the Balearic-Algerian basins. In: Kenyon, H., Ivanov, M.K., Akhmetzhanov, A.M., Kozlova, E.V. (Eds.), Interdisciplinary Geoscience Studies of the Gulf of Cadiz and Western Mediterranean Basins. IOC Technical Series UNESCO, pp. 48–61.

Corella, J.P., Valero-Garcés, B.L., Moreno, A., Morellón, M., Rull, V., Giralt, S., Rico, M.T., Pérez-Sanz, A., 2011. Sedimentary evolution and palaeohydrology of karstic, meromictic Montcortés Lake (Spanish Pre-Pyrenees) during the last 6,000 years. Journal of Paleolimnology 46 (3), 351–367.

Corella, J.P., in preparation. Climatic and anthropogenic factors influencing sedimentation on karstic Lake Arreo (N Spain) during the last 2,500 years. Quaternary Research.

Desprat, S., Sánchez-Goñi, M.F., Loutre, M.F., 2003. Revealing climatic variability of the last three millennia in northwestern Iberia using pollen influx data. Earth and Planetary Science Letters 213, 63–78.

Détriché, S., Bréhéret, J.G., Soulié-Märsche, I., Karrat, L., Macaire, J.J., 2009. Late Holocene water level fluctuations of Lake Afourgagh (Middle-Atlas mountains, Morocco) inferred from charophyte remains. Palaeogeography, Palaeoclimatology, Palaeoecology 283, 134–147.

Dezileau, L., Sabatier, P., Blanchemanche, P., Joly, B., Swingedouw, D., Cassou, C., Castaings, J., Martinez, P., Von Grafenstein, U., 2011. Intense storm activity during the little Ice Age on the French Mediterranean coast. Palaeogeography, Palaeoclimatology, Palaeoecology 299, 289–297.

Diz, P., Francés, G., Pelejero, C., Grimalt, J.O., Vilas, F., 2002. The last 3000 years in the R|¤a de Vigo (NW Iberian Margin): climatic and hydrographic signals. The Holocene 12, 459–468.

Ejarque, A., Miras, Y., Riera, S., Palet, J.M., Orengo, H., 2010. Testing micro-regional variability in the Holocene shaping of high mountain cultural landscapes: a palaeoenvironmental case-study in the eastern Pyrenees. Journal of Archaeological Science 37, 1468–1479.

Elderfield, H., Ganssen, G.M., 2000. Past temperature and $\delta^{18}O$ of surface ocean waters inferred from foraminiferal Mg/Ca ratios. Nature 405, 442–445.

Esper, J., Frank, D., Büntgen, U., Verstege, A., Luterbacher, J., Xoplaki, E., 2007. Long-term drought severity variations in Morocco. Geophysical Research Letters 34, L17702.

Fisher, D., Wefer, G., 1999. Use of Proxies in Paleoceanography. Examples from the South Atlantic. Springer-Verlag. 735.

Fiúza, A.F.G., 1983. Upwelling pattern off Portugal. In: Suess, E., Thiede, J. (Eds.), Coastal Upwelling: Its Sediment Record. Plenum, pp. 85–98.

Fletcher, W.J., Zielhofer, C., in press. Fragility of Western Mediterranean landscapes during Holocene rapid climate changes. Catena.

Frigola, J., Moreno, A., Cacho, I., Canals, M., Sierro, F.J., Flores, J.A., Grimalt, J.O., Hodell, D.A., Curtis, J.H., 2007. Holocene climate variability in the western Mediterranean region from a deepwater sediment record. Paleoceanography 22.

Frigola, J., Moreno, A., Cacho, I., Canals, M., Sierro, F.J., Flores, J.A., Grimalt, J.O., 2008. Evidence of abrupt changes in Western Mediterranean deep water circulation during the last 50 kyr: a high-resolution marine record from the Balearic Sea. Quaternary International 181, 88–104.

Frogley, M.R., Griffiths, H.I., Heaton, T.H.E., 2001. Historical biogeography and late Quaternary environmental change of Lake Pamvotis, Ioannina (North-Western Greece): evidence from ostracods. Journal of Biogeography 28, 745–756.

Garcia-Orellana, J., Pates, J.M., Masqué, P., Bruach, J.M., Sanchez-Cabeza, J.A., 2009. Distribution of artificial radionuclides in deep sediments of the Mediterranean Sea. Science of The Total Environment 407, 887–898.

Gil García, M.J., Ruiz Zapata, B., Santiesteban, J.I., Mediavilla, R., López-Pamo, E., Dabrio, C.J., 2007. Late Holocene environments in Las Tablas de Daimiel (south central Iberian peninsula, Spain). Vegetation History and Archaeobotany 16, 241–250.

Giorgi, F., 2006. Climate change hot-spots. Geophysical Research Letters 33, 4.

Gómez-Navarro, J.J., Montávez, J.P., Jerez, S., Jiménez-Guerrero, P., Lorente-Plazas, R., González-Rouco, J.F., Zorita, E., 2010. A regional climate simulation over the Iberian Peninsula for the last millennium. Climate of the Past Discussion 6, 2071–2116.

Gray, L.J., Beer, J., Geller, M., Haigh, J.D., Lockwood, M., Matthes, K., Cubasch, U., Fleitmann, D., Harrison, G., Hood, L., Luterbacher, J., Meehl, G.A., Shindell, D., van Geel, B., White, W., 2010. Solar influences on climate. Reviews of Geophysics 48, RG4001.

Heegaard, E., Birks, H.J.B., Telford, R.J., 2005. Relationships between calibrated ages and depth in stratigraphical sequences: an estimation procedure by mixed-effect regression. The Holocene 15, 612–618.

Jiménez-Espejo, F.J., Martínez-Ruiz, F., Sakamoto, T., Ijima, K., Gallego-Torres, D., Harada, N., 2007. Paleoenvironmental changes in the western Mediterranean since the last glacial maximum: high resolution multiproxy record from the Algero-Balearic basin. Palaeogeography, Palaeoclimatology, Palaeoecology 246, 292–306.

Jiménez-Espejo, F.J., Martínez-Ruiz, F., Rogerson, M., González-Donoso, J.M., Romero, O., Linares, D., Sakamoto, T., Gallego-Torres, D., Rueda Ruiz, J.L., Ortega-Huertas, M., Perez Claros, J.A., 2008. Detrital input, productivity fluctuations, and water mass circulation in the westernmost Mediterranean Sea since the last glacial maximum. Geochemistry, Geophysics, Geosystems 9.

Jones, M.D., Roberts, C.N., Leng, M.J., Türkes, M., 2006. A high-resolution late Holocene lake isotope record from Turkey and links to North Atlantic and monsoon climate. Geology 343, 361–364.

Jones, P.D., Briffa, K.R., Osborn, T.J., Lough, J.M., Ommen, T.D.v., Vinther, B.M., Luterbacher, J., Wahl, E.R., Zwiers, F.W., Mann, M.E., Schmidt, G.A., Ammann, C.M., Buckley, B.M., Cobb, K.M., Esper, J., Goosse, H., Graham, N., Jansen, E., Kiefer, T., Kull, C., Küttel, M., Mosley-Thompson, E., Overpeck, J.T., Riedwyl, N., Schulz, M., Tudhope, A.W., Villalba, R., Wanner, H., Wolff, E., Xoplaki, E., 2009. High-resolution palaeoclimatology of the last millennium: a review of current status and future prospects. The Holocene 19, 3–49.

Kaufman, Darrell S., Schneider, David P., McKay, Nicholas P., Ammann, Caspar M., Bradley, Raymond S., Briffa, Keith R., Miller, Gifford H., Otto-Bliesner, Bette L., Overpeck, Jonathan T., Vinther, y Bo M., 2009. Recent warming reverses long-term Arctic cooling. Science 325 (5945), 1236–1239. doi:10.1126/science.1173983.

Last, W.M., Smol, J.P. (Eds.), 2001. Tracking Environmental Change Using Lake Sediments. Kluwer Academic Publishers, Norwell, MA, U.S.A.

Lebreiro, S., Francés, G., Abrantes, F., Diz, P., Bartels-Jonsdottir, H., Stroynowski, Z.N., Gil, I., Pena, L.D., Rodrigues, T., Jones, P.D., Nombela, M.A., Alejo, I., Briffa, K.R., Harris, I., Grimalt, J.O., 2006. Climate change and coastal hydrographic response along the Atlantic Iberian margin (Tagus Prodelta and Muros Ría) during the last two millennia. The Holocene 16, 1003–1015.

Lebreiro, S.M., Voelker, A.H.L., Vizcaino, A., Abrantes, F.G., Alt-Epping, U., Jung, S., Thouveny, N., Gràcia, E., 2009. Sediment instability on the Portuguese continental margin under abrupt glacial climate changes (last 60 kyr). Quaternary Science Reviews 28, 3211–3223.

López-Merino, L., López-Sáez, J.A., Sánchez, F.A., Pérez-Díaz, S., Shaad, D.A., Guerra Doce, y E., 2009. Estudio polínico de una laguna endorreica en Almenara de Adaja (Valladolid, Meseta Norte): cambios ambientales y actividad humana durante los últimos 2800 años. Revista Española de Micropaleontología 41 (3), 333–348.

Luterbacher, J., Xoplaki, E., Dietrich, D., Jones, P.D., Davies, T.D., Portis, D., Gonzalez-Rouco, J.F., von Storch, H., Gyalistras, D., Casty, C., Wanner, H., 2001. Extending North Atlantic oscillation reconstructions back to 1500. Atmospheric Science Letters 2, 114–124.

Magny, M., Arnaud, F., Holzhauser, H., Chapron, E., Debret, M., Desmet, M., Leroux, A., Millet, L., Revel, M., Vannière, B., 2010. Solar and proxy-sensitivity imprints on paleohydrological records for the last millennium in west-central Europe. Quaternary Research 73, 173–179.

Magny, M., Peyron, O., Gauthier, E., Vannière, B., Millet, L., Vermot-Desroches, B., 2011. Quantitative estimates of temperature and precipitation changes over the last millennium from pollen and lake-level data at Lake Joux, Swiss Jura Mountains. Quaternary Research 75, 45–54.

Mangini, A., Spötl, C., Verdes, P., 2005. Reconstruction of temperature in the Central Alps during the past 2000 yr from a [delta]18O stalagmite record. Earth and Planetary Science Letters 235, 741–751.

Mann, M.E., Jones, P.D., 2003. Global surface temperatures over the past two millennia. Geophysical Research Letters 30. doi:10.1029/2003GL017814.

Mann, M.E., Zhang, Z., Rutherford, S., Bradley, R.S., Hughes, M.K., Shindell, D., Ammann, C., Faluvegi, G., Ni, F., 2009. Global signatures and dynamical origins of the little ice age and medieval climate anomaly. Science 326, 1256–1260.

Martín-Chivelet, J., Muñoz-García, M.B., Edwards, R.L., Turrero, M.J., Ortega, A.I., 2011. Land surface temperature changes in Northern Iberia since 4000 yr BP, based on δ13C of speleothems. Global and Planetary Change 77, 1–12.

Martinez-Cortizas, A., Pontedevedra-Pombal, X., Garcia-Rodeja, E., Novoa-Munoz, J.C., Shotyk, W., 1999. Mercury in a Spanish peat bog archive of climate change and atmospheric metal deposition. Science 284, 939–942.

Martín-Puertas, C., Valero-Garcés, B.L., Mata, P., González-Sampériz, P., Bao, R., Moreno, A., Stefanova, V., 2008. Arid and humid phases in southern Spain during the last 4000 years: the Zoñar Lake record, Córdoba. The Holocene 40, 195–215.

Martín-Puertas, C., Jiménez-Espejo, F., Martínez-Ruiz, F., Nieto-Moreno, V., Rodrigo, M., Mata, M.P., Valero-Garcés, B.L., 2010. Late Holocene climate variability in the southwestern Mediterranean region: an integrated marine and terrestrial geochemical approach. Climate of the Past 6, 807–816.

Martín-Vide, J., López-Bustins, J.A., 2006. The western Mediterranean oscillation and rainfall in the Iberian peninsula. International Journal of Climatology 26, 1455–1475.
Masquè, P., Fabrès, J., Canals, M., Sánchez-Cabeza, J.A., Sánchez-Vidal, A., Cacho, I., Calafat, A., Bruach, J.M., 2003. Accumulation rates of major constituents of hemipelagic sediments in the deep Alboran Sea: as centennial perspective of sedimentary dynamics. Marine Geology 193, 207–233.
Millot, C., 1999. Circulation in the western Mediterranean sea. Journal of Marine Systems 20, 423–442.
Miras, Y., Ejarque, A., Riera, S., Palet, J.M., Orengo, H., Euba, I., 2007. Dynamique holocène de la végétation et occupation des Pyrénées andorranes depuis le Néolithique ancien, d'après l'analyse pollinique de la tourbière de Bosc dels Estanyons (2180 m, Vall del Madriu, Andorre). Comptes Rendus Palevol 6, 291–300.
Moore, P.D., Webb, J.A., Collinson, M.E., 1991. Pollen Analysis, second ed. Blackwell Scientific Publications.
Morellón, M., Valero-Garcés, B., Vegas-Vilarrúbia, T., González-Sampériz, P., Romero, Ó., Delgado-Huertas, A., Mata, P., Moreno, A., Rico, M., Corella, J.P., 2009. Lateglacial and Holocene palaeohydrology in the western Mediterranean region: the Lake Estanya record (NE Spain). Quaternary Science Reviews 28, 2582–2599.
Morellón, M., Valero-Garcés, B., González-Sampériz, P., Vegas-Vilarrúbia, T., Rubio, E., Rieradevall, M., Delgado-Huertas, A., Mata, P., Romero, Ó., Engstrom, D.R., López-Vicente, M., Navas, A., Soto, J., 2011. Climate and human signatures during the medieval warm period and the little ice age in the Spanish pre-Pyrenees: the Lake Estanya record. Journal of Paleolimnology 46 (3), 423–452.
Morellón, M., Pérez-Sanz, A., Corella, J.P., Büntgen, U., Catalán, J., González-Sampériz, P., González-Trueba, J.J., López-Sáez, J.A., Moreno, A., Pla-Rabes, S., Saz-Sánchez, M.Á., Scussolini, P., Serrano, E., Steinhilber, F., Stefanova, V., Vegas-Vilarrúbia, T., Valero-Garcés, B., 2012. A multi-proxy perspective on millennium-long climate variability in the Southern Pyrenees. Climate of the Past 8, 683–700. doi:10.5194/cp-8-683-2012.
Moreno, A., Cacho, I., Canals, M., Prins, M.A., Sánchez-Goñi, M.F., Grimalt, J.O., Weltje, G.J., 2002. Saharan dust transport and high latitude glacial climatic variability: the Alboran Sea record. Quaternary Research 58, 318–328.
Moreno, A., Cacho, I., Canals, M., Grimalt, J.O., Sánchez-Goñi, M.F., Shackleton, N.J., Sierro, F.J., 2005. Links between marine and atmospheric processes oscillating at millennial time-scale. A multy-proxy study of the last 50,000 yr from the Alboran Sea (Western Mediterranean Sea). Quaternary Science Reviews 24, 1623–1636.
Moreno, A., Valero-Garcés, B.L., González-Sampériz, P., Rico, M., 2008. Flood response to rainfall variability during the last 2000 years inferred from the Taravilla Lake record (Central Iberian Range, Spain). Journal of Paleolimnology 40, 943–961.
Moreno, A., González-Sampériz, P., Morellón, M., Valero-Garcés, B.L., Fletcher, W.J., 2012. Northern Iberian abrupt climate change dynamics during the last glacial cycle: a view from lacustrine sediments. Quaternary Science Reviews 36, 139–156.
Müller, P.J., Kirst, G., Ruhland, G., von Storch, I., Rosell-Melé, A., 1998. Calibration of the alkenone paleotemperature index $U^{K'}_{37}$ based on core-tops from the eastern South Atlantic and the global ocean (60°N–60°S). Geochimica et Cosmochimica Acta 62 (10), 1757–1772.
Neumann, F.H., Kagan, E.J., Schwab, M.J., Stein, M., 2007. Palynology, sedimentology and palaeoecology of the late Holocene Dead Sea. Quaternary Science Reviews 26, 1476–1498.
Nieto-Moreno, V., Martínez-Ruiz, F., Giralt, S., Jiménez -Espejo, F., Gallego-Torres, D., Rodrigo-Gámiz, M., García -Orellana, J., Ortega-Huertas, M., de Lange, G.J., 2011. Tracking climate variability in the Western Mediterranean during the Late Holocene: a multiproxy approach. Climate of the Past 7, 1395–1414.
Pèlachs, A., Pérez-Obiol, R., Ninyerola, M., Nadal, J., 2009. Landscape dynamics of Abies and Fagus in the southern Pyrenees during the last 2200 years as a result of anthropogenic impacts. Review of Palaeobotany and Palynology 156, 337–349.
Pena, L., Calvo, E., Cacho, I., Eggins, S., Pelejero, C., 2005. Identification and removal of Mn-Mg-rich contaminant phases in foraminiferal tests: Implications for Mg/Ca past temperature reconstructions. Geochemistry Geophysics Geosystems 6.
Pena, L.D., Francés, G., Diz, P., Esparza, M., Grimalt, J.O., Nombela, M.A., Alejo, I., 2010. Climate fluctuations during the Holocene in NW Iberia: high and low latitude linkages. Continental Shelf Research 30, 1487–1496.
Pérez-Sanz, A., González-Sampériz, P., Valero-Garcés, B., Moreno, A., Morellón, M., Sancho, C., Belmonte, A., Gil-Romera, G., Sevilla, M., Navas, A., 2011. Clima y hombre: cambios de la vegetación durante los últimos 2000 años en el Pirineo Central a partir del registro palinológico de la Basa de la Mora. Zubía 23, 17–38.
Pinardi, N., Masetti, E., 2000. Variability of the large scale general circulation of the Mediterranean Sea from observations and modelling: a review. Palaeogeography, Palaeoclimatology, Palaeoecology 158, 153–173.
Proctor, C., Baker, A., Barnes, W., 2002. A three thousand year record of North Atlantic climate. Climate Dynamics 19, 449–454.
Reimer, P., Baillie, M., Bard, E., Bayliss, A., Beck, J., Blackwell, P., Bronk Ramsey, C., Buck, C., Burr, G., Edwards, R., Friedrich, M., Grootes, P., Guilderson, T., Hajdas, I., Heaton, T., Hogg, A., Hughen, K., Kaiser, K., Kromer, B., McCormac, F., Manning, S., Reimer, R., Richards, D., Southon, J., Talamo, S., Turney, C., van der Plicht, J., Weyhenmeyer, C., 2009. IntCal09 and Marine09 radiocarbon age calibration curves, 0–50,000 years cal BP. Radiocarbon 51, 1111–1150.
Rivas-Martínez, S., 2007. Mapa de series, geoseries y geopermaseries de vegetación de España. Memoria del mapa de la vegetación potencial de España. Itineraria Geobotanica 17, 1–436.
Roberts, N., Moreno, A., Valero-Garcés, B.L., Corella, J.P., Jones, M., Allcock, S., Woodbridge, J., Morellón, M., Luterbacher, J., 2012. Palaeolimnological evidence for a bipolar climate see-saw in the Mediterranean since AD900. Global and Planetary Change 84-85, 23–34.
Rodó, X., Baert, E., Comin, F.A., 1997. Variations in seasonal rainfall in Southern Europe during the present century: relationships with the North Atlantic oscillation and the El Niño-southern oscillation. Climate Dynamics 13, 275–284.
Rodrigo-Gámiz, M., Martínez-Ruiz, F., Jiménez -Espejo, F., Gallego-Torres, D., Nieto-Moreno, V., Romero, O., Ariztegui, D., 2011. Impact of climate variability in the western Mediterranean during the last 20,000 years: oceanic and atmospheric responses. Quaternary Science Reviews 30, 2018–2034.
Rodrigues, T., Grimalt, J.O., Abrantes, F.t.G., Flores, J.A., Lebreiro, S.M., 2009. Holocene interdependences of changes in sea surface temperature, productivity, and fluvial inputs in the Iberian continental shelf (Tagus mud patch). Geochemistry, Geophysics, Geosystems 10.
Rull, V., González-Sampériz, P., Valero-Garcés, B., Corella, P., Morellón, M., 2011. Vegetation changes in the southern Pyrenean flank during the last millennium in relation to climate and human activities: the Montcortès lacustrine record. Journal of Paleolimnology 46 (3), 387–404.
Schnurrenberger, D.W., Kelts, K., Johnson, T.C., Shane, L.C.K., Ito, E., 2001. National lacustrine core repository (LacCore). Journal of Paleolimnology 25, 123–127.
Scussolini, P., Vegas-Vilarrúbia, T., Rull, V., Corella, J.P., Valero-Garcés, B., Gomà, J., 2011. Mid-Holocene climate change and human impact based on diatoms, algae and aquatic vegetation pollen from Lake Montcortès. Journal of Paleolimnology 46 (3), 369–385.
Seager, R., Graham, N., Herweijer, C., Gordon, A.L., Kushnir, Y., Cook, E., 2007. Blueprints for medieval hydroclimate. Quaternary Science Reviews 26, 2322–2336.
Shindell, D.T., Schmidt, G.A., Mann, M.E., Rind, D., Waple, A., 2001. Solar forcing of regional climate change during the Maunder Minimum. Science 294, 2149.
Smol, J.P., Birks, H.J., Last, W., 2001a. Tracking environmental change using lake sediments. Terrestrial, algal, and siliceous indicators. In: Smol, J.P. (Ed.), Developments in Paleoenvironmental Research. Springer, Dordrecht, The Netherlands, p. 400.
Smol, J.P., Birks, H.J., Last, W., 2001b. Tracking environmental change using lake sediments. Zoological indicators. In: Smol, J.P. (Ed.), Developments in Paleoenvironmental Research. Springer, Dordrecht, The Netherlands, p. 240.
Solomon, S., Qin, D., Manning, M., Chen, Z., Marquis, M., Averyt, K.B., Tignor, M., Miller, H.L., 2007. Climate Change 2007: The Physical Science Basis. In: Contribution of Working Group I to the Fourth Assessment Report of the Intergovernmental Panel on Climate Change. Cambridge University Press, Cambridge, UK.
Sumner, G., Homar, V., Ramis, C., 2001. Precipitation seasonality in eastern and southern coastal Spain. International Journal of Climatology 21, 219–247.
Thorndycraft, V.R., Benito, G., 2006. The Holocene fluvial chronology of Spain: evidence from a newly compiled radiocarbon database. Quaternary Science Reviews 25, 223–234.
Trigo, R.M., Palutikof, J.P., 2001. Precipitation scenarios over Iberia: a comparison between direct GCM output and different downscaling techniques. Journal of Climate 14, 4442–4446.
Trigo, R.M., Osborn, T.J., Corte-Real, J.M., 2002. The North Atlantic oscillation influence on Europe: climate impacts and associated physical mechanisms. Climate Research 20, 9–17.
Trigo, R.M., Pozo-Vázquez, D., Osborne, T., Castro-Díez, Y., Gómiz-Fortis, S., Esteban-Parra, M.J., 2004. North Atlantic oscillation influence on precipitation, river flow and water resources in the Iberian peninsula. International Journal of Climatology 24, 925–944.
Trouet, V.r., Esper, J., Graham, N.E., Baker, A., Scourse, J.D., Frank, D.C., 2009. Persistent positive North Atlantic oscillation mode dominated the medieval climate anomaly. Science 324, 78–80.
Trouet, V., Scourse, J.D., Raible, C.C., 2012. North Atlantic storminess and Atlantic meridional overturning circulation during the last millennium: reconciling contradictory proxy records of NAO variability. Global and Planetary Change 84–85, 48–55.
Valero-Garcés, B., Navas, A., Mata, P., Delgado-Huertas, A., Machín, J., González-Sampériz, P., Moreno, A., Schwalb, A., Ariztegui, D., Schnellmann, M., Bao, R., González-Barrios, A., 2003. Sedimentary facies analyses in lacustrine cores: from initial core descriptions to detailed palaeoenvironmental reconstructions. A case study from Zoñar Lake (Cordoba province, Spain). In: Valero-Garcés, B. (Ed.), Limnogeology in Spain: A Tribute to Kerry Kelts. C.S.I.C., Madrid, pp. 385–414.
Valero-Garcés, B.L., Moreno, A., Navas, A., Mata, P., Machín, J., Delgado-Huertas, A., González-Sampériz, P., Schwalb, A., Morellón, M., Cheng, H., Edwards, R.L., 2008. The Taravilla Lake and tufa deposits (Central Iberian range, Spain) as paleohydrological and paleoclimatic indicators. Palaeogeography, Palaeoclimatology, Palaeoecology 259, 136–156.
van der Weijden, C.H., 2002. Pitfalls of normalization of marine geochemical data using a common divisor. Marine Geology 184, 167–187.
Velasco, J.P.B., Baraza, J., Canals, M., 1996. La depresión periférica y el lomo contourítico de Menorca: evidencias de la actividad de corrientes de fondo al N del Talud Balear. Geogaceta 20, 359–362.

Vicente-Serrano, S., López-Moreno, J.I., 2006. The influence of atmospheric circulation at different spatial scales on winter drought variability through a semi-arid climatic gradient in northeast Spain. International Journal of Climatology 26, 1427–1453.

Vicente-Serrano, S.M., Trigo, R.M., López-Moreno, J.I., Liberato, M.L.R., Lorenzo-Lacruz, J., Beguería, S., Morán-Tejeda, E., Kenawy, A.E., 2011. The 2010 extreme winter north hemisphere atmospheric variability in Iberian precipitation: anomalies, driving mechanisms and future projections. Climate Research 46, 51–65.

Villanueva, J., Pelejero, C., Grimalt, J.O., 1997. Clean-up procedures for the unbiased estimation of C_{37} alkenone sea surface temperatures and terrigenous *n*-alkane inputs in paleoceanography. Journal of Chromatography 757, 145–151.

Wanner, H., Brönnimann, S., Casty, C., Gyalistras, D., Luterbacher, J., Schmutz, C., Stephenson, D.B., Xoplaki, E., 2001. North Atlantic oscillation-concepts and studies. Surveys in Geophysics 22, 321–382.

Wanner, H., Beer, J., Bütikofer, J., Crowley, T.J., Cubasch, U., Flückiger, J., Goosse, H., Grosjean, M., Joos, F., Kaplan, J.O., Küttel, M., Müller, S.A., Prentice, I.C., Solomina, O., Stocker, T.F., Tarasov, P., Wagner, M., Widmann, M., 2008. Mid- to Late Holocene climate change: an overview. Quaternary Science Reviews 27, 1791–1828.

Wick, L., Lemcke, G., Sturm, M., 2003. Evidence of Lateglacial and Holocene climatic change and human impact in eastern Anatolia: high-resolution pollen, charcoal, isotopic and geochemical records from the laminated sediments of Lake Van, Turkey. The Holocene 13, 665–675.